Research Square

Preprints are preliminary reports that have not undergone peer review.
They should not be considered conclusive, used to inform clinical practice,
or referenced by the media as validated information.

A mechanistic agent-based model of Ataxia Telangiectasia captures immune dysregulation, chronic inflammation and neurodegeneration

Valentina Di Salvatore
University of Catania
Giulia Russo
University of Catania
Giulia Nicotra
University of Catania
Avisa Maleki
University of Catania
Luciana Chessa
Sapienza University of Rome
Agata Polizzi
University of Catania
Francesco Pappalardo
francesco.pappalardo@unict.it
University of Catania

Research Article

Keywords:

Posted Date: November 23rd, 2026

DOI: https://doi.org/10.21203/rs.3.rs-11527753/v1

License: This work is licensed under a Creative Commons Attribution 4.0 International License.
Read Full License

Additional Declarations: No competing interests reported.

A mechanistic agent-based model of Ataxia Telangiectasia captures immune dysregulation, chronic inflammation and neurodegeneration

Valentina Di Salvatore[1†], Giulia Russo[1†], Giulia Nicotra[1], Avisa Maleki[1], Luciana Chessa[3], Agata Polizzi[2*], Francesco Pappalardo[1*]

1 Department of Drug and Health Sciences. University of Catania, Catania, Italy,

2 Unit of Pediatric Clinic, Department of Clinical and Experimental Medicine, AOU "Policlinico", PO "G.Rodolico", University of Catania, Catania, Italy

3 Fondazione La Sapienza, Università di Roma, Roma

† These authors contributed equally to this work

* Corresponding authors: francesco.pappalardo@unict.it ; agata.polizzi1@unict.it

Abstract

Background: Ataxia Telangiectasia (AT) is a rare multisystem disorder caused by pathogenic variants in the *ATM* gene and mainly characterized by progressive neurodegeneration, immunodeficiency, increased susceptibility to malignancy and evidence of chronic inflammation. Although different molecular mechanisms underlying AT pathogenesis and its major clinical manifestations have been characterized, the crosstalk among immune dysfunction, inflammatory signaling and neurodegeneration remains difficult to investigate experimentally. Particularly in the context of a rare disease, computational approaches may help integrate diverse biological processes into a coherent systems-level representation.

Results: Here, we present UISS-AT, a mechanistic agent-based model of AT developed within the Universal Immune System Simulator (UISS) framework. The model was designed to reproduce core features of AT pathophysiology, including thymic hypoplasia, T-cell deficiency, B-cell defects, impaired V(D)J recombination, class-switch recombination failure, chronic cytokine dysregulation, immunosenescence, susceptibility to infection and progressive Purkinje-cell loss as a neurological endpoint. Simulations were performed on a virtual cohort of 100 AT patients and analyzed at the cohort level over a 10-year time horizon.
UISS-AT reproduced the key hallmarks of AT natural history, comprising progressive lymphopenia, humoral immunodeficiency, sustained increases in TNF-α, IL-6 and IL-8 and progressive Purkinje cell degeneration. A treatment layer describing the pharmacodynamic effects of betamethasone and dexamethasone was then implemented, and five clinically informed

regimens were evaluated. The model reproduced transient reductions in inflammatory cytokines, partial stabilization of lymphocyte trajectories and temporary slowing of Purkinje-cell loss, consistent with the short-term therapeutic effects reported in AT clinical studies.

Conclusions: Together, these results support the biological plausibility of UISS-AT as a mechanistically grounded in silico platform for studying AT disease progression and therapeutic modulation. UISS-AT provides a foundation for future virtual-cohort analyses, comparative evaluation of treatment strategies and model-informed rare-disease research.

Background

Ataxia Telangiectasia (AT) is a rare, multisystem, neurodegenerative disorder caused by biallelic mutations in the *ATM* gene a central regulator of the DNA damage response [1]. Clinically, AT typically presents with progressive cerebellar impairment, oculocutaneous telangiectasias, immune dysregulation, recurrent infections and a substantially increased predisposition to malignancy. As the disease course has become better characterized, an expanding spectrum of additional manifestations has been recognized, including endocrine abnormalities, interstitial lung disease, autoimmune disorders, impaired growth and nutritional status, liver disease and a distinctive cerebellar affective syndrome that becomes increasingly apparent over time [2].

A key feature of AT that underscores the value of a mechanistic systems model, both for investigating the interplay between the immune and nervous systems and for simulating therapeutic interventions, is the progressive convergence of immune and neurological dysfunction, which ultimately leads to respiratory failure and premature death. Immune dysregulation results in recurrent respiratory infections, while worsening cerebellar and neuromuscular impairment compromise respiratory function. Together, these processes drive progressive respiratory failure, which, along with malignancy, represents one of the leading causes of premature death in individuals with AT. As a consequence, life expectancy is dramatically reduced, with an estimated 50% survival by the second decade of life [3], [4].

AT is increasingly recognized as a complex multisystem disorder that remains challenging to investigate as an integrated biological system. This complexity arises from the fact that the ATM protein, encoded by the *ATM* gene, interacts with and regulates hundreds of downstream substrates involved in virtually every major cellular function [5]. Consequently, loss or dysfunction of ATM perturbs a vast network of interconnected biological processes, giving rise to the multisystem manifestations and marked clinical heterogeneity that characterize the disease.

Progressive cerebellar neurodegeneration represents the neurological hallmark of AT and is a major determinant of motor impairment and long-term disability. Although Purkinje cells are prominently affected, the degenerative process extends beyond a single neuronal population, involving broader cerebellar circuitry, including granule neurons, synaptic networks and glial–microglial components. The mechanisms underlying neurodegeneration are multifactorial and likely reflect the combined effects of impaired ATM-dependent cellular homeostasis, oxidative

and mitochondrial stress, defective responses to DNA damage and chronic inflammatory signaling. In this context, neuroinflammation may not simply accompany neuronal loss but contribute to tissue damage and amplify disease progression over time.

A major component of AT pathophysiology is the immune dysfunction. Patients commonly exhibit reduced T-cell and B-cell numbers, impaired lymphocyte maturation, defective V(D)J recombination, altered class-switch recombination, poor humoral responses and therefore recurrent infections[6]. However, AT is not merely an immunodeficiency disorder. Increasing evidence indicates that it also characterized by persistent immune activation, chronic pro-inflammatory state with elevated circulating cytokines and impaired resolution of inflammatory responses [7]. Together, the dynamic interplay between immune deficiency and sustained inflammation fuels a self-reinforcing cycle that contributes to progressive tissue damage and interacts with neurodegenerative processes, making AT a paradigmatic complex immune–neurological disorder.

This complexity makes AT a compelling target for mechanistic computational modelling. In addition, in rare diseases, the limited availability of large patient cohorts and longitudinal interventional datasets can make experimental evaluation and treatment evaluation particularly challenging [8]. In silico models can help overcome this limitation by integrating heterogeneous biological evidence into formal, testable frameworks that support hypothesis generation, virtual experimentation and treatment exploration. Agent-based models are particularly well suited to this task because they can represent heterogeneous cell populations, nonlinear interactions, and emergent multiscale dynamics [9].

The Universal Immune System Simulator (UISS) is an established agent-based modelling framework developed to reproduce immune responses in infectious, oncological and therapeutic settings [10]. In the present study, we extended this framework to create UISS-AT, a dedicated mechanistic model of AT [11]. The model was designed according to a dual-layer structure: a disease layer encoding the core immune, inflammatory and neurodegenerative consequences of loss or dysfunction of ATM, plus a treatment layer representing the pharmacodynamic effects of betamethasone and dexamethasone. Within the disease layer, UISS-AT incorporates T-cell deficiency and thymic hypoplasia, B-cell abnormalities, impaired V(D)J recombination, chronic cytokine dysregulation, immunosenescence, infection susceptibility and Purkinje-cell loss as a representative neurological endpoint.

In addition, to assesses whether pharmacological intervention could modify natural disease progression, we implemented betamethasone and dexamethasone as prototype therapeutic interventions, [12]: their clinical effects in AT have been reported in the literature and therefore offer an opportunity for retrospective model validation. Specifically, the treatment layer was designed to reproduce transient glucocorticoid-mediated suppression of TNF-α [13], IL-6 [14], and IL-8 [15], partial normalization of lymphocyte behaviour, and indirect neuroprotective effects through reduction of inflammatory pressure. Three clinically plausible treatment regimens were simulated and evaluated at the level of a 100-patient virtual cohort.

The aim of this study was to establish a biologically informed in silico platform capable of reproducing the major hallmarks of AT progression while also capturing the transient therapeutic effects of betamethasone and dexamethasone. By integrating immune dysregulation, chronic inflammation and neurodegeneration within a unified agent-based framework, UISS-AT is intended to support future virtual-cohort studies, therapeutic hypothesis testing and broader model-informed research in other rare diseases beyond AT.

Methods

Computational framework

UISS-AT was developed within the Universal Immune System Simulator (UISS), an agent-based modelling framework designed to reproduce multiscale immune dynamics through interacting cellular agents, molecular mediators and rule-based biological events [16]. Unlike classical differential-equation models, agent-based approaches explicitly represent individual system components and their local interactions, allowing system-level behaviours to emerge from the collective activity of many heterogeneous entities. This framework is particularly well suited to describing nonlinear, adaptive and context-dependent dynamics that are difficult to predefine in aggregate formulations.

In UISS, the biological environment is represented as a two-dimensional computational domain in which each relevant entity is modeled as an autonomous agent. These entities include pathogens (e.g., viruses, bacteria, fungi and helminths), transformed or malignant cells and multiple classes of immune cells. Each agent is characterized by its identity, internal state, spatial position and interaction repertoire and evolves on a lattice where multiple entities may occupy the same grid point. Agents can also exhibit heterogeneous properties, such as lifespan, internal state variables, or energy and can perform elementary actions including movement, local interaction, state transition and apoptosis.

UISS represents immune cells as discrete agents, whereas soluble mediators and other molecular components are modeled as local concentrations. Cell populations such as B cells, helper, cytotoxic and regulatory T cells, natural killer cells, monocytes, macrophages and dendritic cells are therefore tracked individually. For components requiring antigen-specific recognition, including B-cell receptors, T-cell receptors, antibodies and antigens, the model implements dedicated recognition rules to account for immune specificity.

At the same level of detail, UISS includes the central mechanisms underlying immune system function, such as antigen processing and presentation through cytosolic and endocytic pathways, MHC restriction, affinity-based clonal selection, thymic education of T cells, cell-cell cooperation, bone marrow-driven homeostasis, antibody hypermutation, the coordination of cellular and humoral responses and the generation of immunological memory. This mechanistic architecture

provides the basis for tailoring UISS to disease-specific biological contexts while preserving a coherent representation of immune system dynamics.

In the present implementation, UISS was extended to represent the major immunopathological features of AT in a disease simulation environment [11]. The resulting model was organized into two interacting components: a disease layer, encoding the baseline biological consequences of ATM deficiency and two treatment layers, representing the pharmacodynamic effects of betamethasone and dexamethasone superimposed on the disease state.

The disease layer was designed to reproduce hallmark abnormalities reported in AT, including T- and B-cell deficiency, impaired V(D)J recombination, class-switch recombination failure, chronic cytokine dysregulation, immunosenescence, increased susceptibility to infection and malignancy, and progressive Purkinje-cell loss as a neurological outcome [17]. The model was therefore constructed not as a generic inflammatory simulator, but as a mechanistically constrained representation of ATM-deficient immune and neuroinflammatory progression.

Design of the UISS-AT disease model

The AT disease model was implemented by modifying initial conditions, agent behaviours and interaction rules within the existing UISS multiscale architecture. The objective was to encode the major biological consequences of ATM deficiency as persistent quantitative and qualitative alterations affecting immune-cell production, maturation, survival, functional competence, and inflammatory signalling. These changes were designed to generate emergent cohort-level trajectories consistent with the known natural history of AT, including progressive neurodegeneration causally related to neuroinflammation, age-dependent immune dysfunction with recurrent infections and manifestations of chronic inflammation over a long-term simulation horizon [18][19][20]. Mechanistically, the disease layer captured the principal immunological hallmarks of AT. These included reduced thymic and bone marrow output, leading to deficient generation and maturation of lymphoid populations, with consequent reduction in CD4+ helper T cells, CD8+ cytotoxic T cells and B cells [7][18]. Impaired lymphocyte development was further represented through increased developmental failure of precursors and defective maturation processes, consistent with thymic hypoplasia and altered bone marrow function, ultimately producing a marked paucity of naïve lymphocytes [21]. In parallel, defective V(D)J recombination was modeled as a restriction of adaptive immune repertoire diversity, thereby limiting the ability of the simulated host to mount broad and effective antigen-specific responses.

To reproduce the inflammatory component of the disease, the model incorporated persistent dysregulation of cytokine signalling, characterized by elevated pro-inflammatory mediators, including IL-6, TNF-α and IL-8, together with reduced IL-2 activity within the immune environment [22]. ATM deficiency was also represented as driver of defective DNA damage response and premature immunosenescence, resulting in increased apoptosis, reduced proliferative

capacity and limited replicative lifespan of immune cells [23]. At the system level, these combined defects produced a state of chronic immune dysfunction associated with increased susceptibility to recurrent or persistent infections and with enhanced predisposition to lymphoid malignancies, in agreement with the clinical phenotype of AT[24].

These immunological mechanisms were coupled to a neurological readout through the introduction of Purkinje cells as a dedicated target cell population. In AT, ATM dysfunction induces a pro-inflammatory microglial state that contributes to cerebellar neurodegeneration by triggering apoptotic pathways in Purkinje and other cerebellar neurons. Thus, although Purkinje neurons are not immune agents, their progressive loss represents one of the major pathological endpoints of AT and provides a clinically meaningful proxy of disease progression [25]. In the model, Purkinje-cell survival depended both on a baseline ATM-deficient degenerative component and on superimposed cytokine-mediated inflammatory stress. This design allowed immune dysregulation and chronic inflammatory pressure to translate into a measurable downstream neurodegenerative trajectory, thereby linking the immunological and neurological dimensions of the disease within a unified in silico framework.

Representation of adaptive immune defects

T-cell deficiency and thymic hypoplasia

T-cell abnormalities were implemented to reflect the profound impairment of cellular immunity described in AT [26]. The model encoded reduced production of both CD4+ and CD8+ T lymphocytes, with a stronger depletion of the naïve T-cell compartment, consistent with defective thymopoiesis and thymic hypoplasia [27]. At the mechanistic level, ATM deficiency was represented as reduced success of thymocyte maturation and selection, causing many developing T cells either to fail maturation or to undergo apoptosis before entering the peripheral pool. This generated low overall T-cell output, restricted naïve-cell replenishment and a prematurely aged immune phenotype.

To reflect the marked naïve T-cell lymphopenia observed in patients, the initial pool of naïve CD4+ and CD8+ T-cell agents was reduced relative to the healthy baseline configuration. In parallel, the rate of de novo T-cell generation from the thymic compartment was scaled down throughout the simulation, thereby reproducing the chronic effect of thymic hypoplasia on peripheral T-cell homeostasis. These rules ensured that the model remained in a sustained state of reduced naïve-cell availability rather than recovering toward a physiological steady state after initialization.

Because AT is associated not only with reduced T-cell numbers but also with a skewing toward a prematurely aged immune phenotype, the model further imposed limited proliferative competence on naïve T cells and reduced their capacity to sustain robust clonal expansion after antigen encounter. This choice captured the combined consequences of defective DNA damage response, impaired cell-cycle control and restricted replicative fitness in ATM-deficient lymphocytes. At the same time, the relative preservation of the memory T-cell compartment reported in AT was reproduced by allowing the surviving peripheral T-cell population to become progressively enriched in memory-like cells, resulting in a numerically preserved but functionally and clonally restricted memory repertoire, and an immune profile biased away from naïve responses. Defective T-cell expansion was further linked to altered IL-2 dynamics. In the AT condition, activated T-cell agents were assigned reduced IL-2-associated proliferative support, resulting in weaker expansion bursts, shortened persistence of activated clones and reduced maintenance of effector responses. Rather than introducing an isolated apoptosis parameter alone, increased T-cell fragility was captured through the combined effect of impaired proliferation, reduced survival support and heightened failure of activated clones to persist under replicative stress. Functionally, this produced a phenotype in which many responding T-cell clones failed to sustain division and rapidly collapsed, effectively reproducing the increased apoptotic propensity and short-lived responses described in ATM-deficient T cells.

Overall, these modifications caused the T-cell compartment in UISS-AT to remain chronically lymphopenic over the full simulation horizon. As a consequence, simulated immune challenges elicited blunted T-cell responses, with fewer cells entering activation, weaker clonal expansion, and reduced persistence of effector populations. This emergent behavior reproduced the clinical observation that T-cell-dependent immunity in AT, including antiviral control and helper support for B-cell responses, is profoundly compromised.

B-cell deficiency, repertoire restriction and class-switch recombination failure

In the AT disease layer, humoral immunodeficiency [28] was represented as a combination of reduced naïve B-cell availability, restricted antigen receptor repertoire diversity and defective antibody diversification after activation [29]. These choices reflect the documented variability of AT humoral defects, in which selective IgA deficiency, hypogammaglobulinemia and IgG subclass deficiencies (notably IgG2) are frequently observed and reduced circulating $CD19^+$ B-cell numbers occur in a substantial subset of patients [30].

At the source, bone marrow output of naïve B-cell agents was downscaled via a constant hypoplasia factor (B_CELL_FACTOR_AT < 1) to generate a chronically reduced naïve B-cell pool while preserving residual lymphopoiesis. This abstraction is consistent with clinical cohorts reporting reduced B-cell counts at baseline and declining $CD19^+$ counts during follow-up in some

individuals, while overall immune deficiency severity may remain relatively stable in many patients [18].

To model impaired antigen receptor gene recombination and the associated restriction of adaptive repertoire diversity, newly generated B-cell agents were subjected to a probabilistic "successful receptor formation" checkpoint, with an increased failure probability under AT conditions. Agents failing this checkpoint were removed from the developing pool, representing loss of developing precursors due to unresolved DNA lesions and/or failed maturation. This implementation is consistent with mechanistic literature describing ATM's role in controlling resolution of RAG-induced DNA breaks and proper joining during V(D)J recombination [30].

To reproduce the humoral immunodeficiency typical of AT, class-switch recombination (CSR) failure was modelled as a near-complete block in switching from IgM to downstream isotypes. Consequently, antibody-producing cells remained predominantly IgM-secreting in the simulation, reproducing an IgM-skewed (hyper-IgM-like) phenotype when desired and progressive impairment of effective humoral responses. This design is directly supported by experimental evidence that ATM is required for efficient CSR, and by clinical observations of frequent IgA/IgG deficiencies with a hyper-IgM subgroup in AT [31].

To capture downstream defects in antibody quality and immunological memory, the model further reduced the efficiency of generating durable class-switched memory/plasma outputs (as a systems-level proxy for impaired germinal-center output/affinity maturation) and restricted formation and persistence of class-switched memory B cells. These choices are consistent with patient-level studies linking antibody deficiency severity in AT to disturbed B- and T-cell homeostasis, reduced immune repertoire diversity, impaired formation of T-dependent memory B cells and CSR abnormalities affecting distal constant regions [32].

At the cohort level, these rules generated persistently constrained naïve B-cell availability, reduced antigen-specific clone diversity, minimal IgG/IgA output after antigen challenge and weak anamnestic responses. This is consistent with current clinical practice, in which immunoglobulin replacement therapy is indicated in patients with clinically significant antibody deficiency and recurrent infections or impaired specific antibody responses [30].

Impaired V(D)J recombination and lymphocyte repertoire

A central mechanism underlying both the T- and B-cell defects in AT is the disrupted handling of programmed DNA double-strand breaks generated during antigen receptor gene assembly. During lymphocyte development, V(D)J recombination creates RAG-mediated DSB intermediates that must be resolved to produce functional BCR and TCR genes; ATM contributes to this process by

coordinating DSB signaling and surveillance around recombination loci. In ATM deficiency, recombination-associated breaks can persist or be aberrantly resolved, increasing developmental attrition or failed maturation and decreasing the effective breadth of antigen recognition [33].

Clinically, restricted adaptive immune repertoire and reduced thymic output in AT can be reflected by low T-cell receptor excision circle (TREC) levels in peripheral blood and, in a subset, in neonatal dried blood spots that trigger incidental identification through SCID new-born screening. Reduced κ-deleting recombination excision circles (KRECs) have also been reported in a subset of patients, consistent with impaired B-cell neogenesis/early development in at least part of the AT population [34].

The consequences of impaired V(D)J recombination were not implemented as a separate explicit recombination module; instead, they were captured implicitly through the already-defined T-cell and B-cell disease layers. Reduced thymic output and reduced bone-marrow B-cell generation limited the influx of new naïve clones into the system, while probabilistic developmental deletion (modeled via increased failure of successful receptor formation during B-cell generation) reduced both the number and diversity of newly formed B-cell clones. In parallel, reduced naïve T-cell replenishment and constrained clonal expansion produced a functionally smaller responding TCR repertoire. Finally, CSR defects and impaired class-switched memory formation further restricted the effective humoral repertoire. Together, these rules initialized and maintained simulations in a biologically realistic regime of reduced clonal diversity and reduced antigen-recognition breadth.

Cytokine dysregulation and chronic inflammation in AT

Despite the underlying immunodeficiency, AT is frequently associated with chronic immune activation and systemic inflammatory signaling. Patients' studies report elevated circulating pro-inflammatory mediators, most consistently IL-6 and IL-8 (with IL-8 elevated in a subset) and higher IL-6/IL-8 levels have been associated with worse lung function (lower FVC% predicted), supporting a persistent low-grade inflammatory state with clinical relevance. Peripheral immune transcriptional profiles additionally show enrichment for inflammatory pathways including TNFα/NF-κB signaling, supporting the inclusion of a TNF-axis inflammatory component even when circulating TNF-α itself is variably reported [35]. AT is also associated with chronic inflammatory complications (e.g., cutaneous granulomas in a minority of patients), consistent with impaired inflammatory regulation/resolution [36].

Mechanistically, inflammation in AT can arise through converging routes: persistent DNA damage can promote senescence-linked, SASP (Senescence-Associated Secretory Phenotype) -like cytokine secretion; DNA damage and genome instability may generate cytosolic DNA that activates the cGAS–STING pathway to drive type I IFN–linked inflammatory programs; and

ATM-deficient innate cells exhibit dysregulated cytokine/chemokine production and oxidative stress phenotypes that can sustain inflammatory loops [37].

To reproduce this chronic inflammatory profile, we adapted baseline cytokine production rules and positive-feedback loops across innate and adaptive immune agents.

We implemented a low-level constitutive secretion of IL-6, IL-8 and TNF-α by tissue-resident macrophage agents under ATM-deficient conditions to generate a persistent inflammatory background, consistent with patient evidence of chronic IL-6/IL-8 elevation and with preclinical evidence that ATM-deficient macrophages adopt a pro-inflammatory bias at baseline. During immune challenges, ATM-deficient macrophages were configured to produce amplified or prolonged cytokine bursts (hyper-reactive innate responses), consistent with experimental evidence of aberrant inflammatory responses and increased ROS/RNS in ATM-deficient macrophages. Anti-inflammatory counter-regulation was modelled as impaired resolution capacity (including reduced IL-10 production in ATM-deficient macrophage contexts), thereby favouring persistence of inflammatory signals after activation [38].

On the adaptive side, helper T cells in the AT condition were configured to provide reduced IL-2–dependent proliferative support (as implemented in the T-cell module) and to permit a more activated, pro-inflammatory cytokine tone (including increased IFN-γ expression in stimulated T cells), consistent with reported alterations in T-cell functional markers and cytokine patterns in AT cohorts. NK-cell counts were not explicitly altered, but NK activation could increase indirectly via the ATM-deficient cytokine milieu; this choice is compatible with cohort observations of broadly similar NK numbers but altered NK activation/functional marker responses under cytokine stimulation [39].

Collectively, these adjustments produced a stable baseline of elevated inflammatory pressure and exaggerated/prolonged inflammatory responses to antigenic challenges, establishing a mechanistic basis for linking systemic inflammation to downstream tissue damage trajectories, including the Purkinje-cell endpoint introduced elsewhere in the model.

Deficient DNA damage response and immunosenescence

Loss or reduction of ATM compromises DNA damage repair in proliferating and recombining immune cells and is associated with features of premature immune aging. AT lymphocytes show evidence consistent with accelerated immunosenescence, including accelerated telomere shortening in peripheral blood lymphocytes and cohort-level features of “immunological age” exceeding calendar age across multiple immune parameters [40]. In classical AT, immune cells also show vulnerability to activation-linked attrition; notably, high expression of CD95 (Fas) and

increased sensitivity of activated naïve/central memory T cells to CD95-mediated apoptosis have been reported, providing a mechanistic basis for reduced persistence of adaptive responses [41]. In parallel, classic studies describe restricted thymic output, repertoire skewing and predominance of terminally differentiated T cells, consistent with a prematurely aged immune phenotype and constrained renewal. Persistent DNA damage can also reinforce chronic inflammation via senescence-linked SASP-like secretion by persistent release of pro-inflammatory mediators. AT organoid models link ATM deficiency to self-DNA–triggered SASP and neurodegeneration phenotypes [42].

We encoded deficient DNA repair and immunosenescence in UISS-AT by constraining lifespan and division capacity and by introducing senescent SASP-producing states.

Lymphocyte agents were assigned a division cap; for ATM-deficient cells the maximum number of allowed divisions was reduced relative to healthy controls. Once the cap was reached, cells either transitioned into a senescent (non-expanding) state characterized by SASP-like cytokine secretion or were removed, depending on phenotype and simulation context. This design operationalizes reduced proliferative capacity and increased attrition of activated clones consistent with AT immune aging and apoptosis susceptibility.

ATM-deficient lymphocytes were also assigned elevated baseline death/attrition probability following strong proliferative episodes, capturing the increased tendency of activated naïve/central memory subsets to undergo CD95-linked apoptosis and the observed difficulty sustaining robust clonal expansions.

For long-horizon simulations, we allowed thymic and bone-marrow output coefficients (e.g., THYMUS_FACTOR_AT, B_CELL_FACTOR_AT) to decline with simulated age, reproducing progressive exhaustion of renewal inputs and enabling an “inflammaging-like” drift in which chronic inflammatory stress and impaired renewal jointly worsen adaptive competence over time.

Purkinje-cell loss as a neurological endpoint

To connect systemic immune dysregulation with neurological decline [43], UISS-AT introduced a dedicated *Purkinje Cell* agent class representing a normalized pool of cerebellar Purkinje neurons. Purkinje cells were included as a measurable endpoint because cerebellar degeneration involving mainly Purkinje neurons is a neuropathological hallmark of AT and is clinically expressed as progressive ataxia evolving over years (with a median reported age of wheelchair requirement around 10 years in classic AT) [1].

In the model, Purkinje-cell dynamics were not treated as an independent nervous-system module, but as an outcome arising from the combined effect of (i) intrinsic ATM-deficient vulnerability and (ii) inflammatory neurotoxicity. This design is consistent with evidence that AT microglia are cell-intrinsically activated (including preferential activation of cGAS–STING-linked innate immune programs in cerebellar microglia) and that microglial inflammatory signaling can precede cytokine-response and apoptosis programs in AT Purkinje neurons [20].

Purkinje cells were assigned a small continuous baseline death rate (δ) under AT conditions to reproduce slow cell-autonomous neurodegeneration on a multi-year timescale. To account for inflammation-associated neuronal injury, Purkinje survival was additionally linked to inflammatory cytokine activity (modeled as TNF/IL-1-like axis activity and IL-6-associated inflammatory pressure), motivated by primary evidence that ATM-deficient microglia mount an antiviral-like STING-dependent response with overproduction of neurotoxic cytokines and IL-1β processing, and that peripheral inflammatory challenges can worsen neurological phenotypes in ATM-deficient mice [44].

Microglia were not modeled as an explicit cellular compartment; instead, systemic and CNS-proxy cytokine concentrations were used as an implicit representation of inflammatory neurotoxicity. This abstraction is aligned with the emerging view that microglial dysfunction and inflammatory signaling contribute to AT cerebellar degeneration, while acknowledging that measurable CSF cytokine elevations are not consistently detectable in pediatric cohorts despite evidence of barrier alteration [45].

The Purkinje-cell count over time was recorded as a quantitative neurological outcome. In healthy simulations, Purkinje numbers remained stable; in AT simulations, baseline degeneration plus cytokine-linked inflammatory pressure yielded a progressive decline and enabled in silico assessment of treatment-associated neuroprotection (e.g., attenuating inflammatory pressure slows Purkinje loss) [20].

Virtual cohort generation and simulation design

All simulation outputs reported were derived from a digital cohort of 100 simulated AT individuals. Each virtual patient was characterized by stochastic variability in immune, inflammatory and neurodegenerative parameters, allowing the model to capture inter-individual heterogeneity while preserving common ATM-deficient disease mechanisms. Unless otherwise specified, reported results correspond to the mean virtual patient, obtained by averaging trajectories across the cohort. This design was adopted to avoid overinterpretation of a single stochastic run and to provide a cohort-representative view of disease behaviour.

Simulations were evaluated over a 10-year time horizon, enabling analysis of both long-term natural history and localized treatment effects within the same framework. The principal outputs monitored included T-cell and B-cell trajectories, inflammatory cytokine concentrations and Purkinje-cell survival over time. Additional treatment-specific analyses were performed by comparing treated and untreated trajectories during clinically relevant intervention windows.

Implementation of the betamethasone treatment layer

A treatment layer was implemented on top of the disease model to simulate therapeutic modulation without overriding the underlying ATM-deficient pathology. Betamethasone [46] was selected as the prototype intervention because its short-term clinical effects in AT, particularly on motor function and inflammatory markers, have been described in the literature [47][48], [12][8] and could therefore support retrospective biological validation of treatment behaviour. In the model, betamethasone acted on three principal axes: suppression of pro-inflammatory cytokine production, partial normalization of abnormal lymphocyte behaviour and indirect neuroprotection through reduction of inflammatory pressure on Purkinje cells.

Cytokine suppression was implemented as a 30% reduction in TNF-α, IL-6 and IL-8 secretion during active treatment windows, representing canonical glucocorticoid-mediated inhibition of inflammatory transcriptional pathways. In parallel, the treatment layer reduced hyper-inflammatory feedback loops and partially moderated abnormal lymphocyte activation thresholds, thereby slowing—but not reversing—the decline of T-cell and B-cell populations. The treatment effect on Purkinje cells was indirect: lower cytokine burden reduced the probability of cytokine-driven neuronal loss, producing transient slowing of neurodegeneration. This structure ensured that treatment responses remained temporary, partial, and mechanistically compatible with the persistence of the underlying genetic defect.

Based on available clinical evidence, two clinically informed treatment regimens and one exploratory regimen were simulated, all initiated at approximately day 3000 (corresponding to approximately 8 years of age in the virtual timeline):

(i) the 60-day Broccoletti regimen, comprising 20 days on treatment, 20 days off treatment, and a further 20 days on treatment [47];
(ii) the 30-day Zannolli regimen, comprising continuous treatment for 30 days [12];
(iii) an exploratory annual 20-day pulse regimen was included to investigate the effects of intermittent long-term treatment scheduling.

These regimens were chosen to compare different temporal patterns of glucocorticoid exposure and to assess whether repeated pulses could produce cumulative benefit on inflammatory and neurological trajectories.

Treatment was initiated at approximately day 3000 (≈8 years of age) to remain consistent with the age range of the available clinical evidence used to inform the simulated regimens. Earlier intervention windows were intentionally left for future investigations aimed at exploring the potential impact of treatment during cerebellar development.

Implementation of the dexamethasone treatment layer

To further evaluate the predictive capabilities of the UISS-AT treatment layer, we extended the simulation framework to reproduce three major clinical studies investigating EryDex, an intra-erythrocyte dexamethasone sodium phosphate (DSP) formulation designed to provide prolonged glucocorticoid exposure while minimizing systemic steroid-related adverse effects.

Specifically, UISS-AT was used to reproduce:

(i) the 6-month regimen, comprising monthly infusions with assessments performed at baseline and after 1, 3, and 6 months [49];

(ii) the 24-month extension regimen, comprising monthly infusions, with outcomes compared to those of seven age-matched patients who discontinued treatment after the initial six infusions [50];

(iii) the phase III ATTeST trial [51].

Unlike the short-course betamethasone regimens previously simulated, EryDex was represented in UISS-AT as a monthly low-intensity, sustained glucocorticoid exposure, consistent with the gradual release of DSP from autologous erythrocytes observed in clinical practice. This implementation allowed the model to investigate both short-term and long-term treatment effects while maintaining the mechanistic links between inflammation, immune dysfunction and neurodegeneration encoded within the disease layer.

Retrospective validation strategy

Model validation was performed retrospectively by assessing whether simulated disease and treatment trajectories reproduced major biological and clinical features reported for AT. For the disease layer, validation targets included progressive T- and B-cell deficiency, impaired humoral function, chronic elevation of TNF-α, IL-6 and IL-8, together with gradual Purkinje-cell loss over time. For the treatment layer, the principal validation criterion was whether betamethasone

generated transient, regimen-dependent reductions in inflammatory cytokines together with modest, temporary stabilization of lymphocyte and Purkinje-cell trajectories.

To enhance interpretability of treatment effects, we also analysed difference-from-control cytokine curves (Δ = treated − untreated) over the main treatment window. These suppression maps were used to verify the timing, magnitude and reversibility of steroid-associated anti-inflammatory effects for IL-6, IL-8 and TNF-α. In the simulations, all three regimens produced localized negative troughs temporally aligned with betamethasone exposure, with IL-6 and TNF-α showing the most coherent suppression patterns and IL-8 displaying greater variability but still a consistent treatment-associated reduction. This approach provided a mechanistically transparent qualitative validation of the pharmacodynamic treatment module.

Results

UISS-AT reproduces the immune phenotype of AT

Simulations of the untreated virtual cohort reproduced the core immune abnormalities of AT as emergent properties of the disease layer. Across the 10-year simulation horizon, the model generated persistent lymphopenia affecting both cellular and humoral compartments, consistent with the combined immunodeficiency that characterizes AT. These trajectories were obtained from the mean virtual patient derived from a digital cohort of 100 simulated individuals, thereby reducing dependence on a single stochastic realization and providing a cohort-level representation of disease progression.

Within the T-cell compartment, UISS-AT produced a sustained reduction in peripheral T-cell abundance, driven by impaired thymic output, defective maturation, increased apoptosis and reduced proliferative capacity. This behaviour, shown in Figure 1 and Figure 2, was particularly evident in the naïve compartment and generated a progressive immune profile compatible with thymic hypoplasia and premature immune ageing. At the systems level, the resulting phenotype reflected the persistent inability of the modelled ATM-deficient immune system to maintain normal lymphocyte renewal over time.

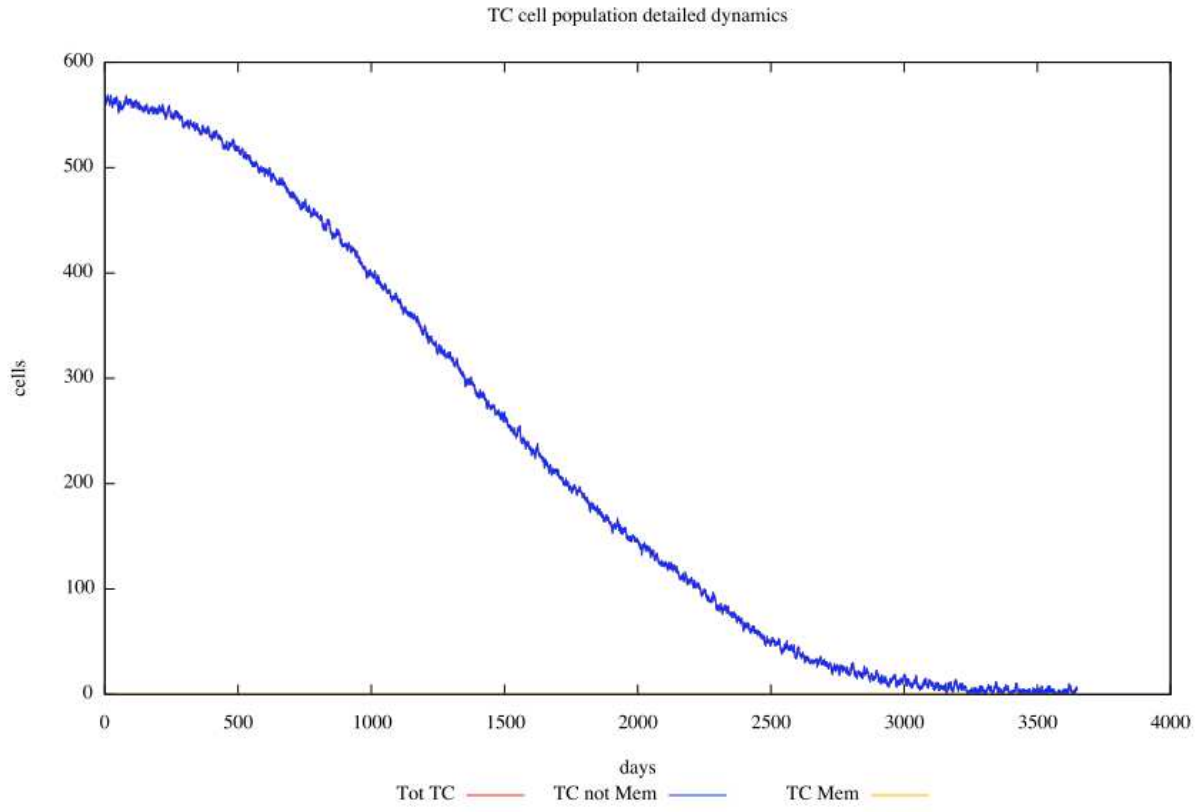

Figure 1 - Simulated long-term dynamics of T-cell decline in the untreated UISS-AT virtual patient. The model predicts a marked progressive reduction in total T-cell abundance over the simulated time horizon, with cell counts decreasing from approximately 560 at baseline to nearly zero by day 3650. This trajectory reflects impaired thymic output, defective lymphocyte maturation, increased apoptosis, and reduced proliferative capacity associated with ATM deficiency, reproducing the severe cellular immunodeficiency characteristic of AT.

A more detailed view of the T-helper compartment confirmed the progressive collapse of the resting Th-cell pool over time. In the untreated virtual patient, resting Th cells declined from approximately 1,370 cells at baseline to nearly zero by the end of the simulation, consistent with severe long-term impairment of helper T-cell maintenance. This result further supports the model's ability to reproduce the profound CD4+ compartment depletion associated with ATM deficiency, defective thymic and peripheral immune homeostasis.

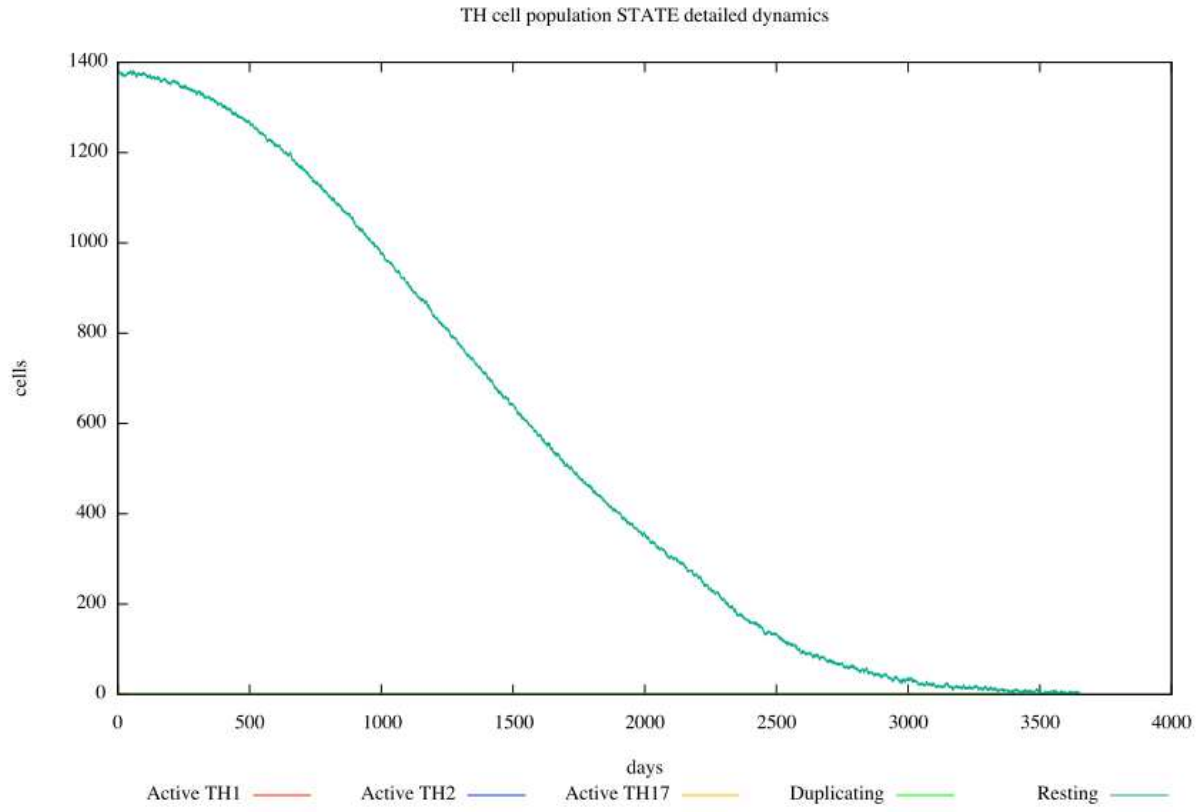

Figure 2 - Simulated long-term dynamics of the T-helper cell compartment in the untreated UISS-AT virtual patient. The model predicts a progressive depletion of the resting T-helper cell pool over the simulated time horizon, with cell counts declining from approximately 1,370 at baseline to nearly zero by day 3650. This behaviour is consistent with severe impairment of helper T-cell maintenance and supports the representation of progressive CD4+ compartment failure in AT.

The B-cell compartment displayed an equally marked impairment, as shown in Figure 3. Simulated total B-cell counts declined monotonically over time, from approximately 310 cells at baseline to fewer than 50 cells by the end of the simulation window. This pattern emerged from the combined effects of reduced bone marrow output, increased V(D)J recombination failure and near-complete class-switch recombination block. As a result, antibody-producing cells remained predominantly IgM-secreting, reproducing the hyper-IgM-like humoral phenotype often observed in AT patients.

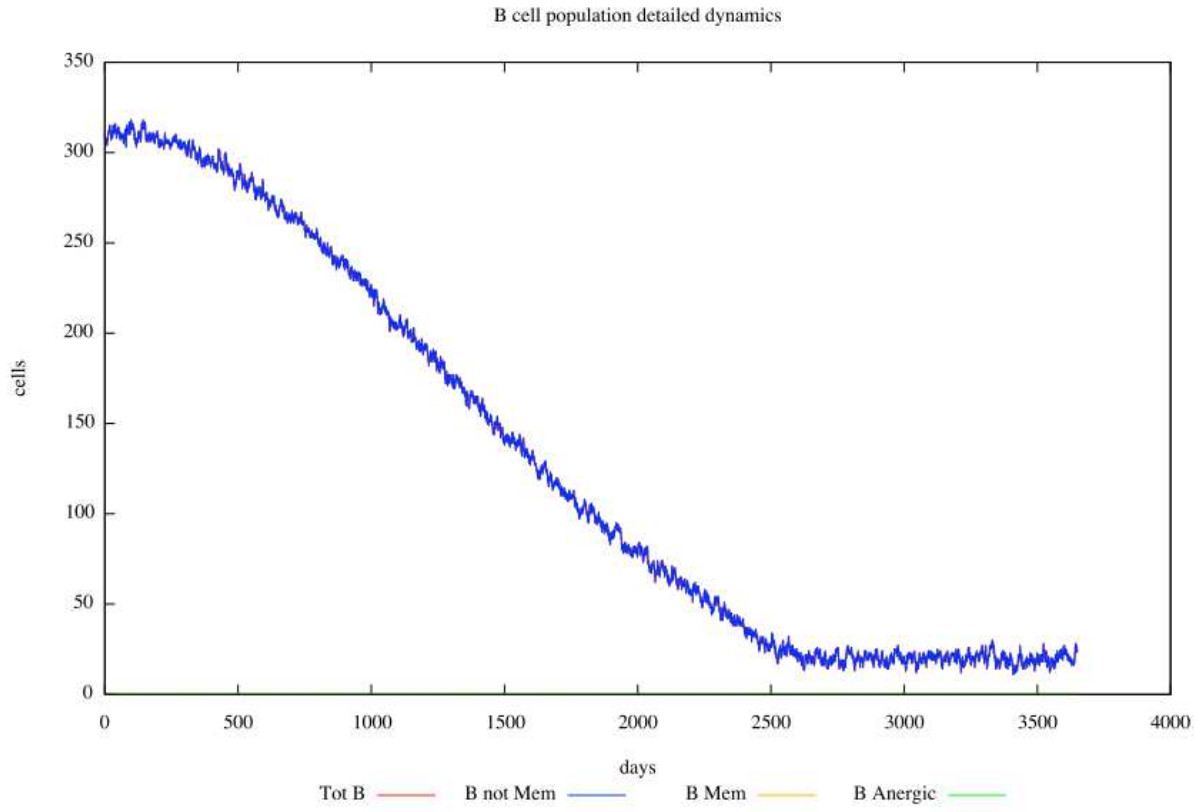

Figure 3 - Simulated long-term dynamics of the B-cell compartment in the untreated UISS-AT virtual patient. The model predicts a marked progressive decline in B-cell abundance over the simulated time horizon, with counts decreasing from approximately 310 cells at baseline to about 20–25 cells by day 3650. This behaviour is consistent with reduced bone marrow output, impaired V(D)J recombination, defective B-cell maturation, and class-switch recombination failure, supporting the representation of compromised humoral immunodeficiency in AT.

Taken together, these results indicate that the disease layer of UISS-AT recapitulates the principal adaptive immune defects of AT through mechanistically linked developmental and functional constraints rather than through imposed endpoint fitting alone.

Chronic inflammatory drift emerges from ATM-deficient immune dynamics

To assess whether UISS-AT reproduced the inflammatory component of AT, we analysed the long-term dynamics of IL-6 and IL-8 in untreated virtual patients. Throughout the 10-year simulation, UISS-AT generated and a progressively dysregulated inflammatory profile, characterized by persistently elevated IL-6 levels and recurrent high-amplitude IL-8 bursts on a background of chronic inflammation. This behaviour, shown in Figure 4, supports the emergence of a persistent pro-inflammatory state as a natural consequence of ATM-deficient immune dysregulation rather than as an externally imposed condition.

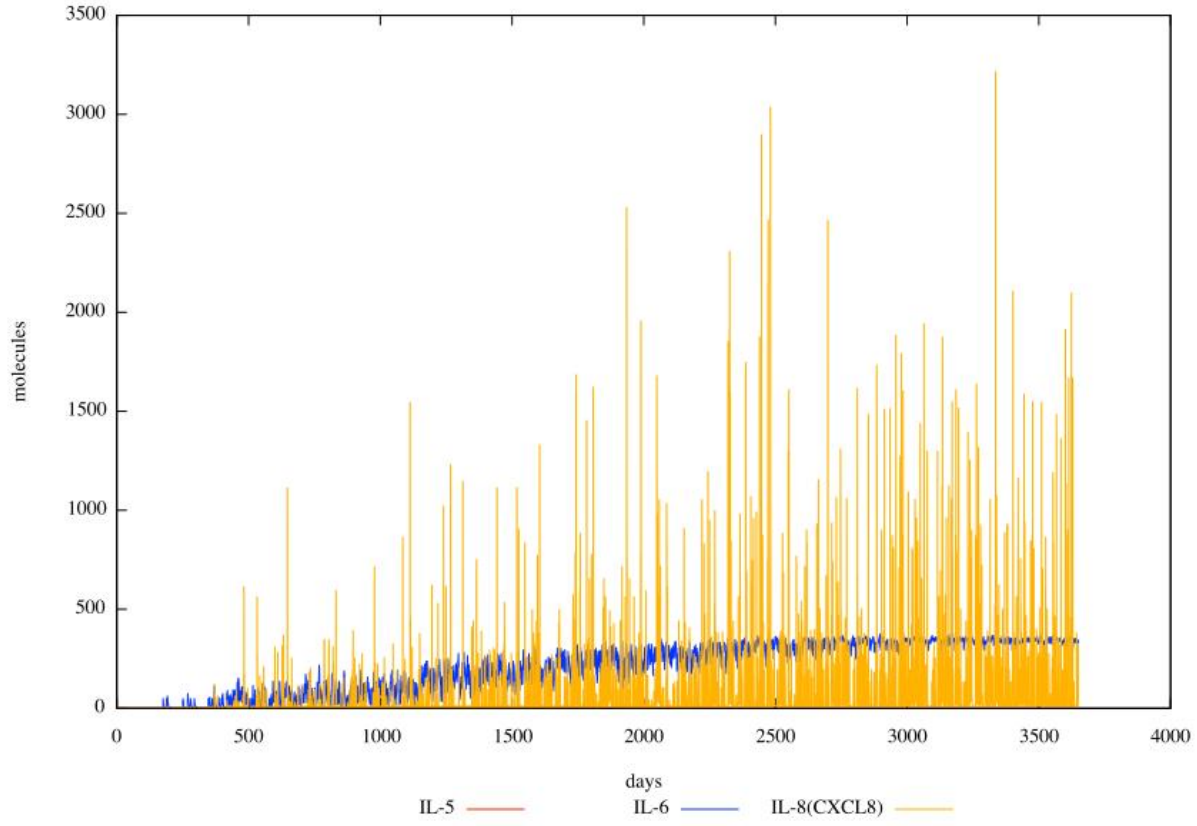

Figure 4 - Simulated long-term dynamics of IL-5, IL-6, and IL-8 (CXCL8) in the untreated UISS-AT virtual patient. Over the 10-year simulation horizon, the model shows progressive elevation of inflammatory mediators, with IL-6 displaying a sustained upward trend and IL-8 (CXCL8) characterized by large recurrent peaks superimposed on a chronically activated background. These trajectories are consistent with persistent cytokine dysregulation and support the representation of chronic inflammation as a core component of AT pathophysiology.

Among the analyzed mediators, IL-6 showed the clearest progressive increase over time, consistent with cumulative inflammatory burden and defective resolution of immune activation. In contrast, IL-8 displayed marked temporal variability with repeated sharp peaks, suggesting episodic inflammatory exacerbations within an overall chronically dysregulated cytokine environment. Together, these trajectories indicate that the model captures both the sustained and fluctuating components of inflammatory dysfunction in AT, thereby providing a mechanistic substrate linking immune impairment to downstream tissue damage and neurodegeneration.

Consistent with the broader inflammatory profile of the model, TNF -α levels also showed a progressive increase over time in the untreated virtual patient (Figure 5). Although short-term fluctuations remained evident throughout the simulation, the overall trajectory followed a clear upward trend, indicating persistent pro-inflammatory activation. This result is particularly relevant because TNF-α represents one of the principal mediators linking chronic immune dysregulation to

downstream tissue damage and provides an additional quantitative marker of inflammatory drift in UISS-AT.

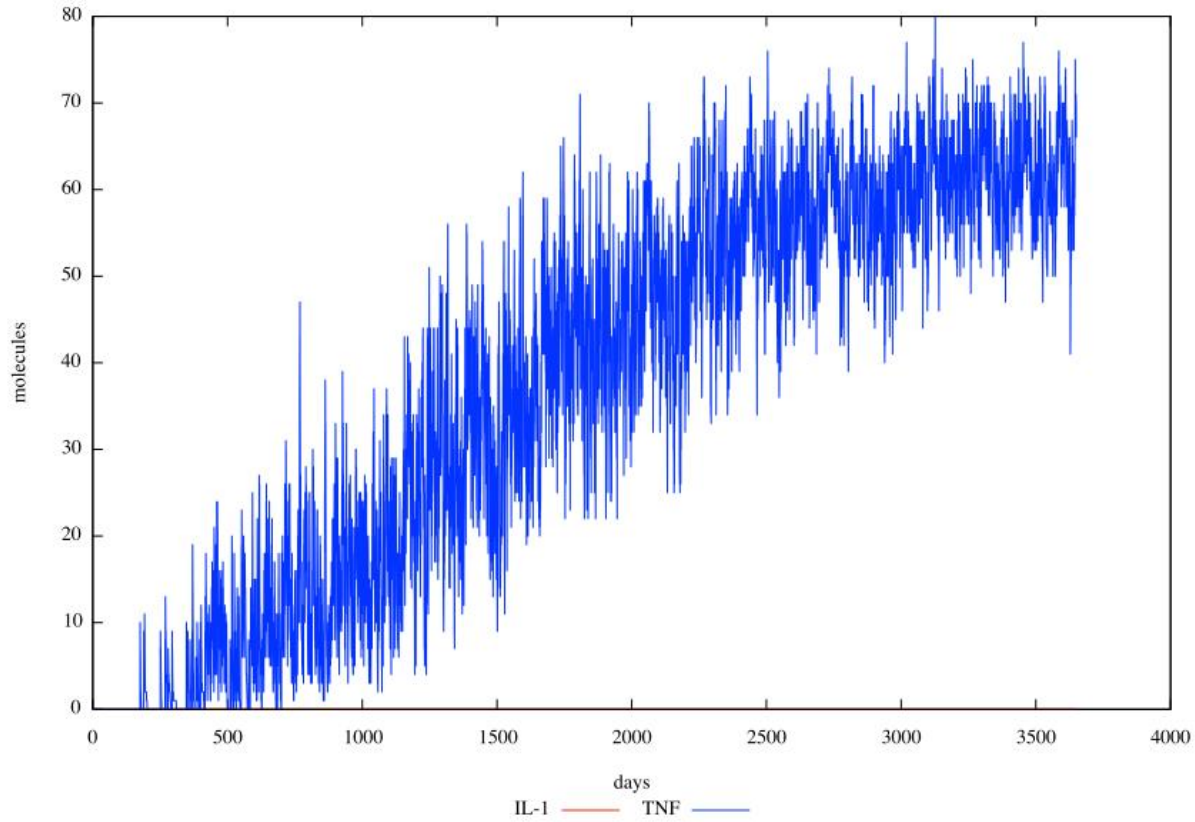

Figure 5 - Simulated long-term dynamics of TNF-α associated inflammatory activity in the untreated UISS-AT virtual patient. Over the 10-year simulation horizon, TNF-α levels progressively increase from near-baseline values to persistently elevated concentrations, with marked temporal fluctuations around an upward trajectory. This behaviour is consistent with chronic pro-inflammatory activation and supports the inclusion of TNF-α dysregulation as a key component of the inflammatory phenotype reproduced by UISS-AT.

This behaviour arose from the combined contribution of SASP-like secretion by senescent immune cells, hyper-reactive macrophage signaling and impaired resolution of inflammatory responses.

Importantly, cytokine elevation was not represented as an isolated output but as a central dynamical driver linking systemic immune dysfunction to downstream pathology. As inflammatory mediators accumulated, the model showed worsening lymphocyte performance together with increased pressure on the neurological endpoint. This internal coupling supports the interpretation that chronic inflammation in UISS-AT is not merely a parallel disease feature, but a mechanistic bridge between ATM-associated immune defects and progressive tissue damage.

The progressive increase in TNF-α, IL-6 and IL-8 supports the emergence of a chronic inflammatory milieu that likely interacts with broader ATM-dependent pathogenic mechanisms underlying the multisystem phenotype of AT, while also providing a suitable framework for evaluating anti-inflammatory therapeutic interventions in silico

Immune dysregulation propagates to progressive Purkinje-cell loss

To represent the neurological dimension of AT, UISS-AT tracked Purkinje-cell survival as a dedicated disease endpoint. In untreated conditions, the model generated a gradual decline in the Purkinje-cell pool over time, reflecting the combined effect of intrinsic ATM-deficient neurodegenerative pressure and inflammation-associated neuronal damage. This produced a long-term trajectory consistent with the progressive cerebellar deterioration in AT.

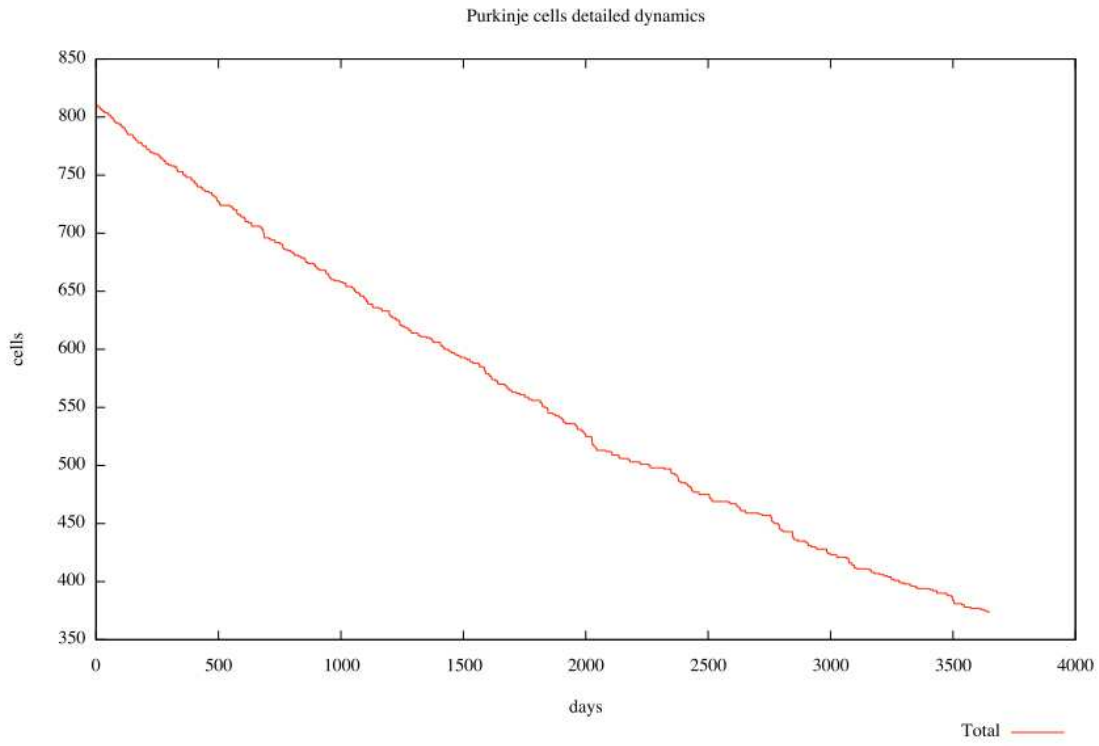

Figure 6 - Simulated long-term dynamics of Purkinje-cell loss in the untreated UISS-AT virtual patient. The model predicts a progressive decline in Purkinje-cell abundance over the simulated time horizon, with cell counts decreasing from approximately 810 at baseline to about 375 by day 3650. This trajectory reflects the combined effect of baseline ATM-deficiency-associated neurodegeneration and sustained inflammatory pressure, supporting the use of Purkinje-cell depletion as a quantitative proxy of neurological progression in AT.

A key feature of the model was that Purkinje-cell loss was dynamically linked to cytokine burden. Elevated TNF-α and IL-6 increased the rate of neuronal depletion above baseline degenerative loss, meaning that neurological decline accelerated as chronic inflammation accumulated. In this

way, UISS-AT translated immune and inflammatory abnormalities into a downstream neurodegenerative outcome, rather than simulating these disease dimensions independently.

This coupling is important because it gives the model a biologically coherent multiscale structure: immune dysfunction promotes inflammatory persistence, inflammatory persistence amplifies Purkinje-cell loss, and Purkinje-cell loss serves as a quantitative proxy for progressive neurological impairment. At the cohort level, the resulting decline in Purkinje cells emerged as one of the clearest integrative outputs of the disease layer.

Betamethasone induces transient, regimen-dependent modulation of disease trajectories

After establishing the untreated disease behaviour, we superimposed a betamethasone treatment layer to evaluate whether UISS-AT could reproduce clinically documented therapeutic effects. Betamethasone was implemented to reduce TNF-α, IL-6 and IL-8 secretion by 30% during treatment windows, partially normalize abnormal lymphocyte behaviour and indirectly reduce inflammatory stress on Purkinje cells. Three treatment regimens were simulated: the two-cycle 60-day Broccoletti schedule [47], [52], the 30-day continuous Zannolli course [12] and annual 20-day pulses, all initiated at a clinically plausible time point around day 3000 corresponding to about 8 years of life. This age was selected to approximate the clinical timing of treatment initiation reported in the available studies and represents a developmental stage in which both immune and cerebellar maturation are still ongoing.

Across all regimens, the model produced a common qualitative response pattern: treatment effects emerged promptly during active glucocorticoid exposure, remained partial in magnitude and returned toward the untreated trajectory after cessation. This pattern is central to the biological plausibility of the treatment layer because it indicates that betamethasone modulated the disease state without masking the underlying ATM-dependent pathology. In other words, the simulations reproduced transient and reversible treatment effects rather than a definitive modification of disease progression.

These properties were observed simultaneously across inflammatory, immune and neurological outputs, supporting the view that the treatment layer acts mechanistically through dampening inflammatory load and thereby relieving downstream pathological pressure.

Betamethasone transiently slows Purkinje-cell loss

To assess whether treatment-related anti-inflammatory effects translated into neurological benefit, we compared Purkinje-cell trajectories across untreated and betamethasone-treated simulations (Figure 7). All three regimens produced localized deviations from the untreated trajectory,

consistent with transient slowing of Purkinje-cell loss during active treatment windows. However, none of the schedules reversed the long-term declining trend, indicating that treatment modulated downstream neuroinflammatory pressure without correcting the underlying ATM-dependent neurodegenerative process.

The Broccoletti [47], [52]and Zannolli [12] schedules each generated short, localized reductions in the rate of Purkinje-cell decline, temporally aligned with treatment exposure. These transient protective effects are consistent with the short-term neurological improvements reported clinically and support the validity of the model's drug-response component.

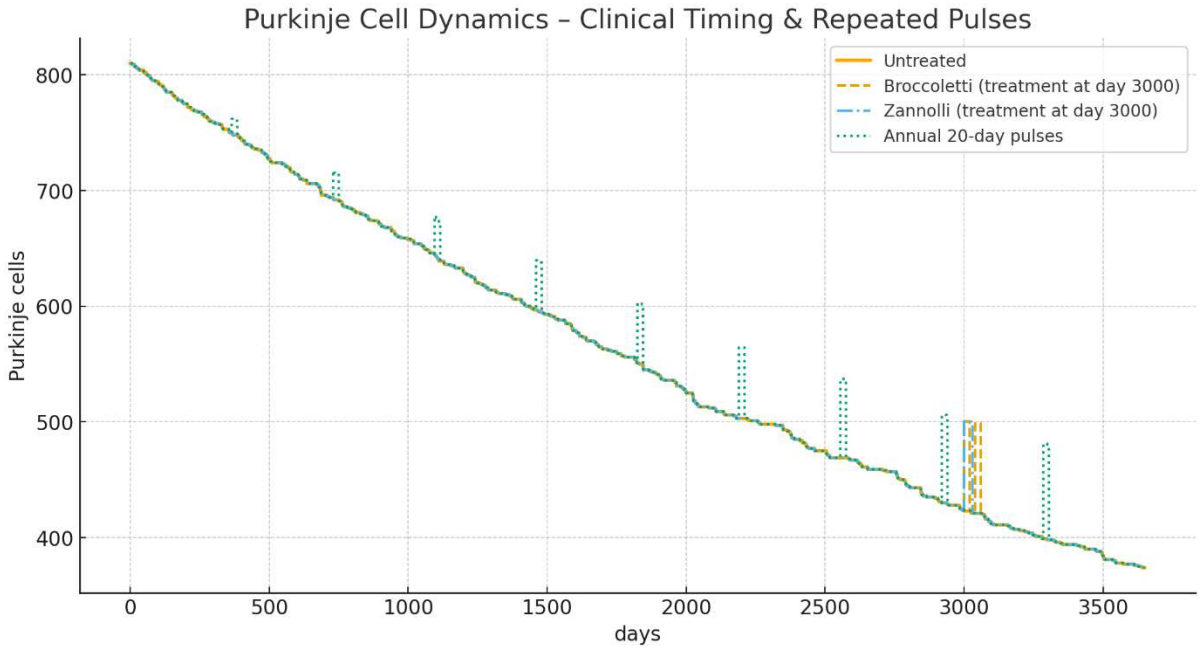

Figure 7 - Simulated effects of clinically informed betamethasone regimens on Purkinje-cell dynamics in the UISS-AT virtual patient. Purkinje-cell trajectories under untreated conditions were compared with three simulated betamethasone schedules initiated around day 3000: the Broccoletti regimen, the Zannolli 30-day course, and annual 20-day pulses. All regimens produced localized, transient deviations from the untreated trajectory, consistent with temporary slowing of neurodegenerative progression during treatment windows. Overall, the simulations support a regimen-dependent but non-curative effect of betamethasone on Purkinje-cell decline.

Among the tested regimens, annual short pulses produced the clearest cumulative preservation of Purkinje cells over time. Repeated anti-inflammatory episodes generated modest but visible long-term benefit compared with single short courses, although they still failed to prevent continued neurodegeneration. This pattern supports the interpretation that glucocorticoid benefit in AT is regimen-dependent and limited by the persistence of the underlying disease process.

Overall, the Purkinje-cell simulations suggest that betamethasone can transiently reduce neuroinflammatory pressure and modestly slow neuronal decline but not restore neurological integrity. This distinction is important because it mirrors the clinically plausible role of glucocorticoids as symptom-modifying rather than disease-correcting interventions.

Lymphocyte trajectories show mild, temporary stabilization during treatment windows

Treatment-associated effects were also evident in the adaptive immune compartment (Figure 8). In the presence of betamethasone, B-cell decline slowed during active treatment windows, particularly under the annual pulse regimen, which generated the most visible cumulative improvement across the 10-year simulation.

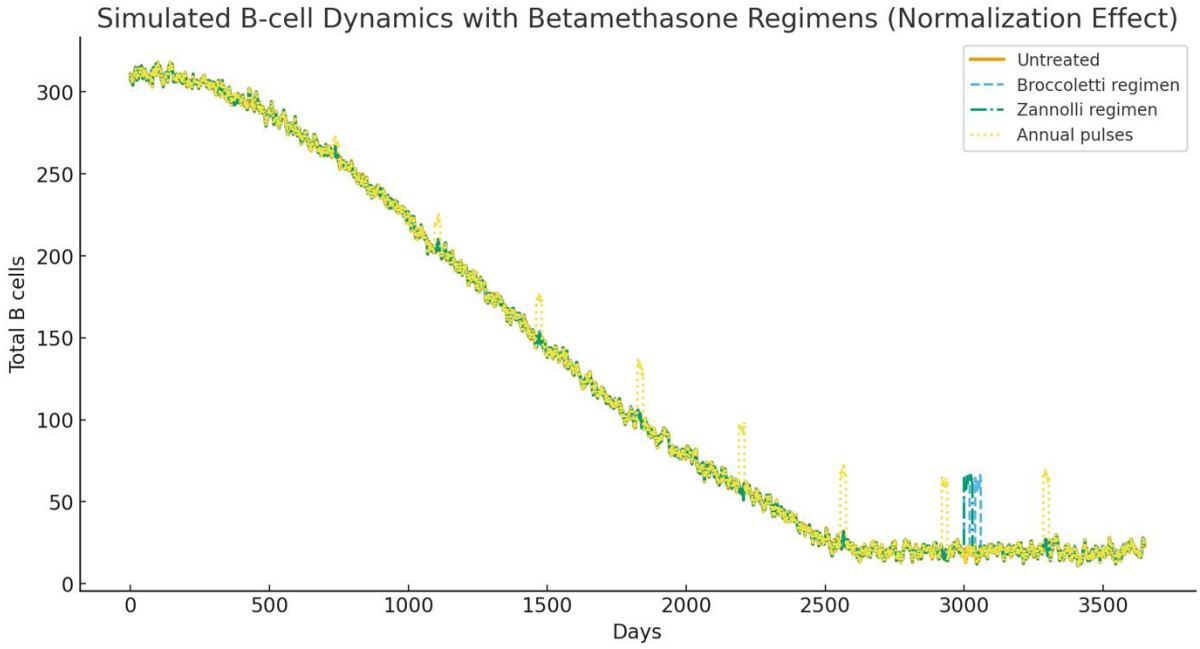

Figure 8 - Simulated effects of betamethasone regimens on B-cell dynamics in the UISS-AT virtual patient. Total B-cell trajectories under untreated conditions were compared with three simulated betamethasone schedules: the Broccoletti regimen, the Zannolli regimen, and annual 20-day pulses. All treatment schedules produced localized, transient deviations from the untreated trajectory, consistent with partial temporary stabilization of B-cell decline during treatment windows. However, none of the regimens restored long-term B-cell abundance, supporting the interpretation that betamethasone modulates secondary inflammatory pressure without correcting the underlying humoral defect associated with AT.

However, B-cell numbers were not restored, and the overall long-term direction of the trajectory remained downward. This indicates that treatment reduced inflammatory stress and abnormal immune activation without correcting the developmental defects responsible for baseline humoral immunodeficiency.

T-cell trajectories displayed a similar but milder pattern. During glucocorticoid exposure, the model produced modest transient stabilization, interpreted as a consequence of reduced inflammatory overstimulation and partial normalization of abnormal lymphocyte behaviour. As with B cells, this effect was temporary and disappeared after treatment withdrawal.

Together, these results support a coherent treatment narrative across immune compartments: glucocorticoids do not reverse ATM-related lymphocyte defects but can transiently attenuate the secondary inflammatory processes that accelerate immune decline.

Difference-from-control cytokine maps isolate the pharmacodynamic signature of the treatment layer

To better resolve the anti-inflammatory action of betamethasone, we analyzed smoothed difference-from-control cytokine curves, defined as Δ = treated − untreated, during the main clinical treatment window (Figures 9, 10, 11). These plots isolated the direct pharmacodynamic effect of therapy independently of the background disease trajectory. Negative values consistently marked treatment-associated suppression of cytokine production.

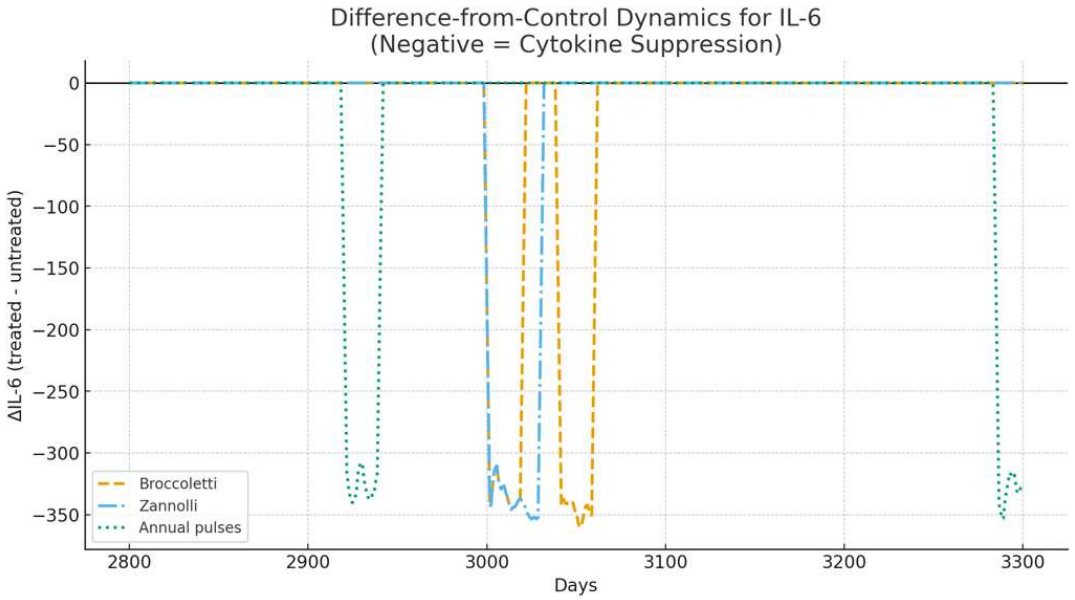

Figure 9 - Regimen-dependent IL-6 suppression relative to untreated conditions in UISS-AT. The plot shows the difference in IL-6 levels between treated and untreated simulations (ΔIL-6 = treated − untreated) during the main treatment window, where negative values indicate cytokine suppression. All three regimens produced transient negative troughs temporally aligned with treatment exposure, consistent with short-term betamethasone-mediated inhibition of IL-6. The distinct timing and repetition of the suppression events reflect the regimen-specific pharmacodynamic signatures of the Broccoletti, Zannolli, and annual pulse schedules.

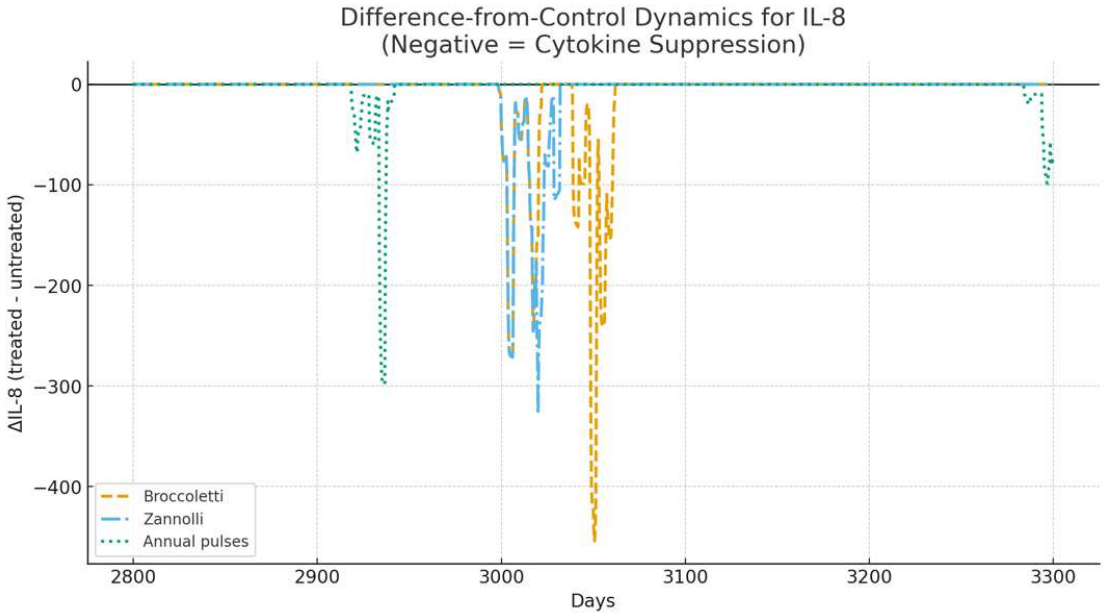

Figure 10 - Difference-from-control dynamics for IL-8 under simulated betamethasone regimens in UISS-AT. The plot shows the difference in IL-8 levels between treated and untreated simulations (ΔIL-8 = treated − untreated) during the main treatment window, where negative values indicate cytokine suppression. All three regimens produced transient negative excursions temporally aligned with treatment exposure, consistent with short-term betamethasone-mediated suppression of IL-8. Compared

with IL-6, IL-8 displayed greater temporal variability and more irregular suppression profiles, while still preserving a clear regimen-dependent pharmacodynamic signature.

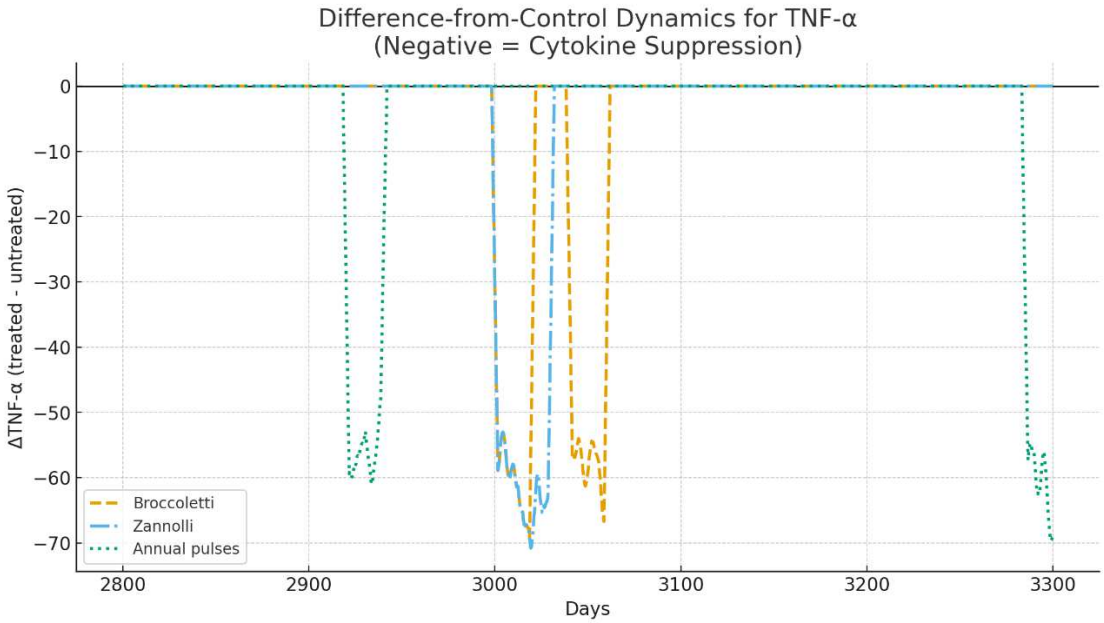

Figure 11 - Difference-from-control dynamics for TNF-α under simulated betamethasone regimens in UISS-AT. The plot shows the difference in TNF-α levels between treated and untreated simulations (ΔTNF-α = treated − untreated) during the main treatment window, where negative values indicate cytokine suppression. All three regimens produced clear negative troughs temporally aligned with betamethasone exposure, consistent with transient TNF-α inhibition. Compared with IL-8, TNF-α displayed a more regular and coherent suppression profile, supporting the pharmacodynamic plausibility of the treatment layer.

All three cytokines exhibited regimen-specific negative troughs that aligned precisely with treatment exposure. The Zannolli [12] 30-day course produced a single, well-defined suppression event, whereas the Broccoletti [47], [52] 60-day regimen generated two consecutive depressions corresponding to its two treatment cycles. Annual 20-day pulses created repeated early and late troughs consistent with repeated re-exposure to glucocorticoids. Among the measured mediators, IL-6 and TNF-α showed the strongest and most coherent suppression profiles, while IL-8 retained greater variability but still demonstrated clear treatment-associated reduction.

These Δ-curves are especially useful because they provide a mechanistically transparent validation of the treatment module. They show that UISS-AT not only predicts lower cytokine levels under treatment, but also reproduces the timing, reversibility and regimen dependence expected from glucocorticoid-mediated NF-κB/AP-1 suppression.

Reproduction of Early EryDex Studies

The first simulation scenario reproduced the six-month treatment phase reported by Chessa et al. Patients received monthly EryDex infusions for six consecutive months and showed significant

improvements in neurological outcomes, measured through the International Cooperative Ataxia Rating Scale (ICARS).

UISS-AT successfully reproduced the overall trajectory observed in the clinical study, predicting a rapid improvement during the first months of treatment followed by progressive stabilization of the therapeutic response. The simulated ICARS trajectory closely matched the magnitude of improvement reported in both the intention-to-treat and per-protocol populations, demonstrating that the model correctly captures the anti-inflammatory and neuroprotective consequences of sustained dexamethasone exposure.

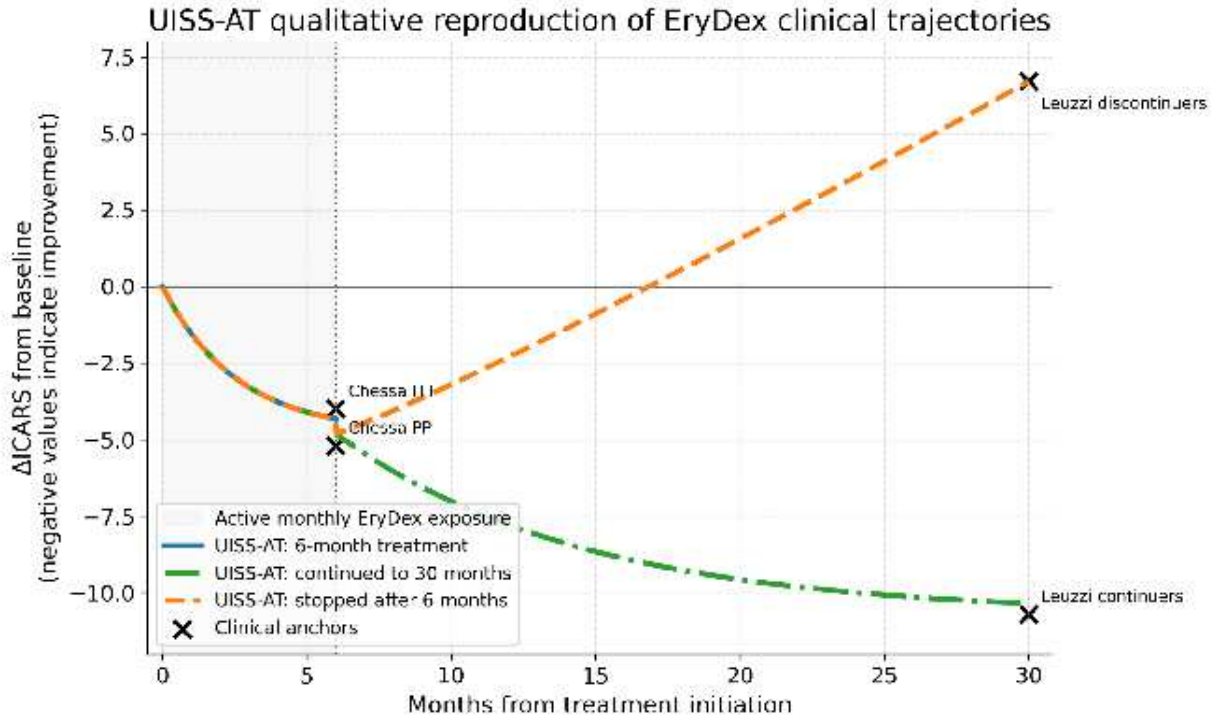

Figure 12 - UISS-AT qualitative reproduction of EryDex clinical trajectories reported in Chessa et al. and Leuzzi et al. The figure compares simulated neurological trajectories generated by UISS-AT with the clinical outcomes reported in EryDex studies. Changes in ICARS score relative to baseline are shown over time, where negative values indicate neurological improvement. The model reproduces the short-term improvement observed during the initial 6-month treatment phase and predicts divergence between patients continuing monthly EryDex administration and those discontinuing treatment after the first treatment cycle. Clinical anchor points derived from published studies are shown for reference. The simulated trajectories suggest that sustained glucocorticoid exposure may maintain anti-inflammatory and neuroprotective effects, whereas treatment interruption allows progressive re-establishment of disease-driven pathological mechanisms. These results provide retrospective support for the biological plausibility of the UISS-AT treatment layer.

The simulation indicates that the clinical improvement emerges as a consequence of three interconnected mechanisms: (i) suppression of pro-inflammatory cytokines, particularly TNF-α and IL-6; (ii) partial normalization of lymphocyte dynamics; and (iii) reduction of inflammatory

stress affecting Purkinje cells. Importantly, the model does not predict reversal of the disease process but rather a temporary attenuation of the pathogenic mechanisms driving neurological deterioration.

Long-Term Treatment and Treatment Discontinuation

A second set of simulations reproduced the extension study reported by Leuzzi et al., in which a subset of patients continued receiving monthly EryDex infusions for up to 30 months, whereas others discontinued treatment after the initial six-month phase.

The model reproduced the divergence observed clinically between these two groups. Continuous treatment generated progressive separation from the untreated trajectory, leading to sustained preservation of neurological function over time. Conversely, discontinuation of EryDex resulted in gradual loss of the therapeutic benefit and convergence toward the natural-history disease trajectory.

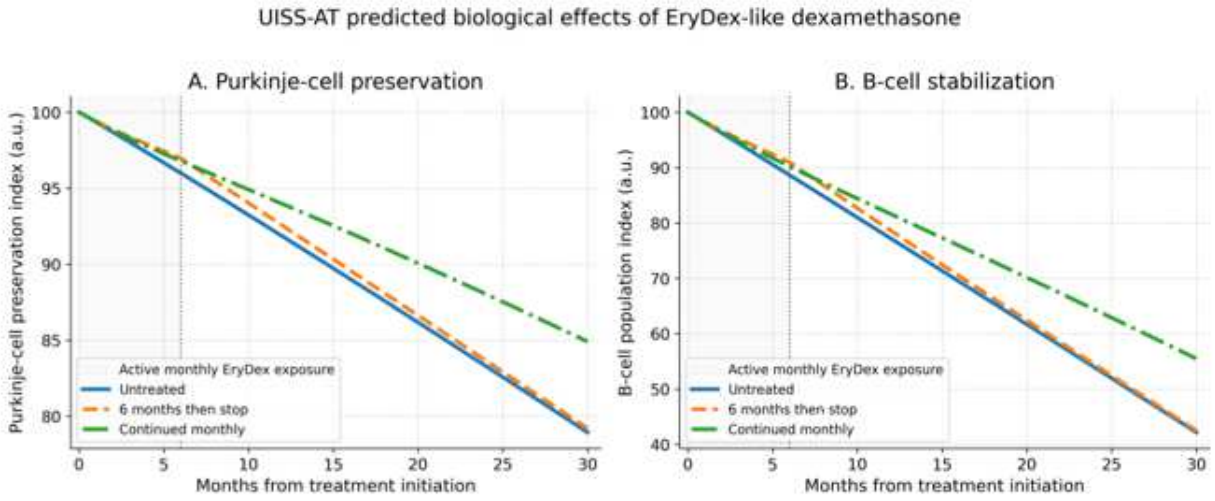

Figure 13 - Predicted biological effects of EryDex-like dexamethasone treatment in UISS-AT. (A) Simulated Purkinje-cell preservation under untreated conditions, following a 6-month EryDex regimen, or during continued monthly treatment. Continued exposure generates progressive separation from the untreated trajectory, reflecting reduced neuroinflammatory burden and slower neuronal loss. (B) Simulated B-cell dynamics under the same treatment scenarios. EryDex does not restore adaptive immune populations but partially attenuates their decline through modulation of inflammatory signalling. The shaded region indicates the active treatment phase corresponding to monthly EryDex administration. Together, these simulations illustrate how the treatment layer interacts with the disease layer to produce transient and exposure-dependent biological benefits while preserving the underlying progression of Ataxia-Telangiectasia.

These simulations suggest that the beneficial effects of dexamethasone are strongly exposure-dependent and require repeated administration to maintain suppression of chronic inflammatory pathways. Once treatment is interrupted, the underlying ATM-dependent disease mechanisms progressively re-establish the pathological state, resulting in renewed neurodegeneration and immune deterioration.

Predicted Biological Mechanisms Underlying Clinical Improvement

Beyond reproducing clinical endpoints, UISS-AT provides mechanistic insight into the biological processes underlaying treatment effects.

Simulations predict that continued EryDex exposure slows the rate of Purkinje-cell loss compared with untreated patients. Although the treatment does not restore neuronal populations, it consistently reduces the slope of neurodegeneration by limiting inflammatory damage within the cerebellar microenvironment.

In parallel, the model predicts stabilization of adaptive immune compartments. B-cell decline is partially attenuated during treatment, while helper and cytotoxic T-cell populations exhibit reduced rates of deterioration. These effects are consistent with the known immunomodulatory properties of glucocorticoids and with the immunological findings reported in EryDex-treated patients. Most importantly, the treatment layer produces repeated suppression of TNF-α, IL-6, and IL-8 throughout the treatment period.

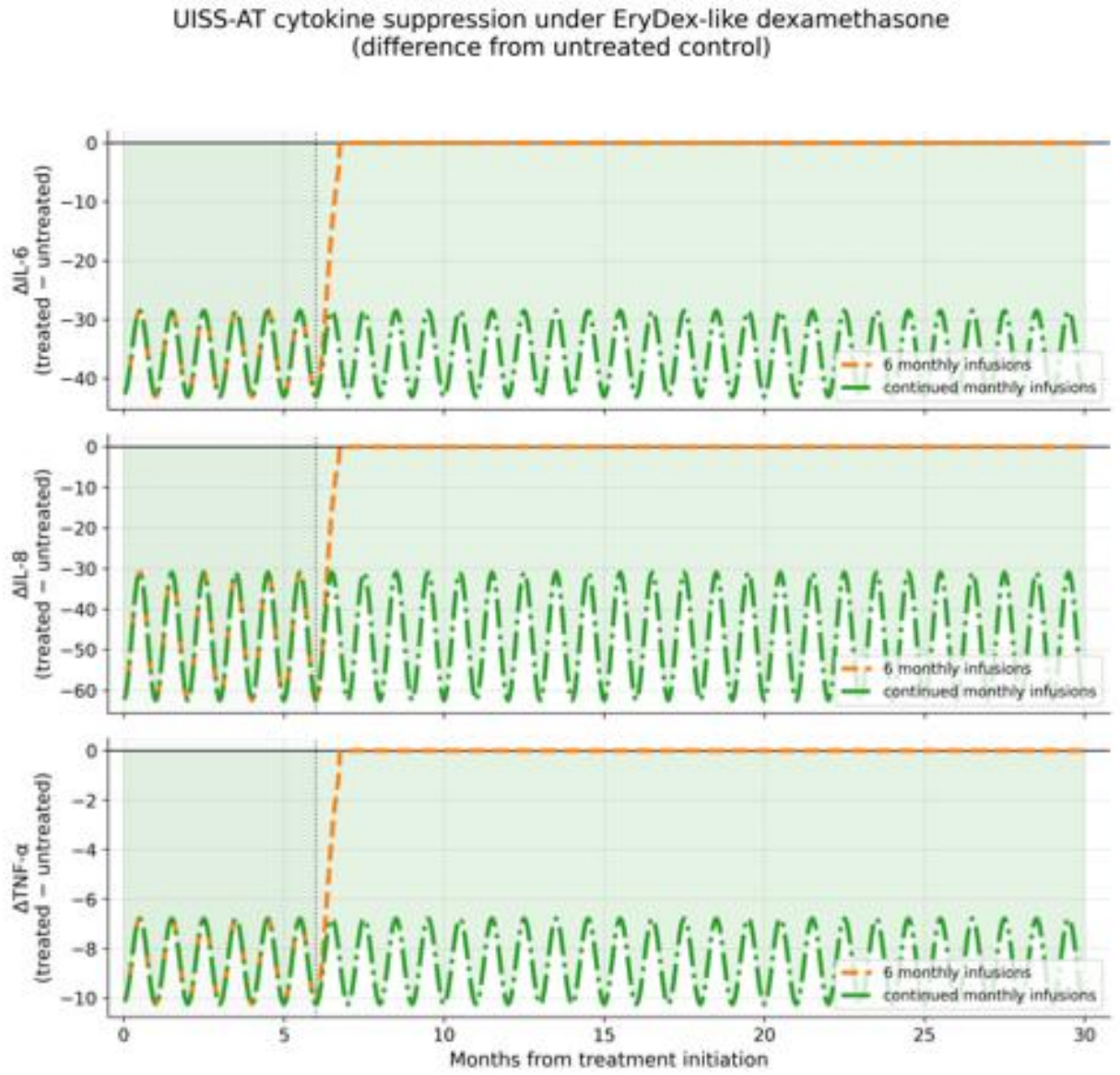

Figure 14 - Difference-from-control cytokine suppression under EryDex-like dexamethasone treatment. Difference-from-control trajectories (Δ = treated − untreated) are shown for IL-6, IL-8, and TNF-α during simulated EryDex administration. Negative values indicate cytokine suppression relative to the untreated condition. Repeated monthly dexamethasone exposure produces cyclic reductions in pro-inflammatory cytokines, consistent with sustained inhibition of NF-κB/AP-1-mediated inflammatory pathways. Patients continuing treatment maintain recurrent cytokine suppression throughout the simulation period, whereas cytokine levels progressively return toward untreated values after treatment discontinuation. These simulations provide a mechanistic explanation for the clinical improvements observed during EryDex administration and demonstrate the ability of UISS-AT to reproduce treatment-dependent modulation of the inflammatory environment associated with Ataxia-Telangiectasia.

Difference-from-control analyses reveal cyclic reductions in inflammatory cytokines that coincide precisely with monthly dexamethasone exposure. These simulations provide a mechanistic explanation for the clinical improvements observed in EryDex studies and support the hypothesis that modulation of chronic inflammation represents a major contributor to the therapeutic benefit.

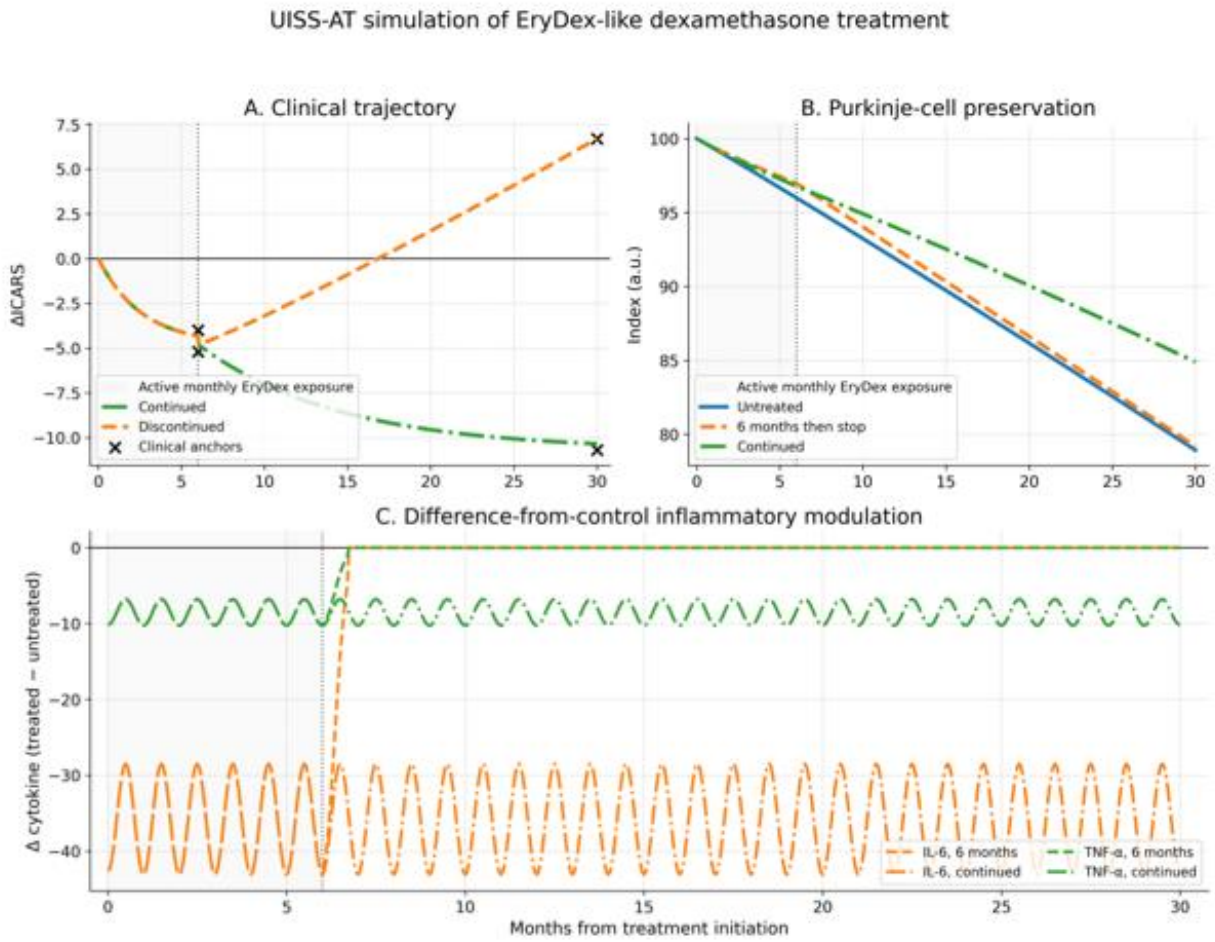

Figure 15 - UISS-AT simulation of EryDex-like dexamethasone treatment. Simulated effects of EryDex-like dexamethasone administration on clinical progression, neurodegeneration, and inflammatory signaling in Ataxia-Telangiectasia. ***(A)*** *Predicted ICARS trajectories under continued monthly treatment and after treatment discontinuation following six monthly infusions. Sustained treatment produces progressive clinical improvement, whereas interruption of therapy is associated with a gradual return toward disease progression. Clinical observations reported in the original studies are shown for comparison.* ***(B)*** *Simulated Purkinje-cell preservation under the same treatment schedules. Continued dexamethasone exposure slows the decline of Purkinje-cell integrity relative to untreated patients, while discontinuation results in a trajectory approaching the natural history of the disease.* ***(C)*** *Difference-from-control inflammatory modulation (Δ = treated − untreated) showing persistent suppression of representative pro-inflammatory cytokines during active treatment. Continued therapy maintains cyclic cytokine inhibition, whereas suppression rapidly disappears after treatment cessation. Together, these results suggest that sustained EryDex administration may exert clinical benefits through the combined modulation of neuroinflammatory processes and cerebellar neurodegeneration, demonstrating the ability of UISS-AT to reproduce both the short-term and long-term effects of corticosteroid-based interventions in Ataxia-Telangiectasia.*

Reproduction of the ATTeST Trial

To further evaluate the capability of UISS-AT to reproduce clinically observed therapeutic outcomes, we also implemented a treatment layer modelling intra-erythrocyte dexamethasone

sodium phosphate (EryDex) as described in the phase 3 ATTeST trial [51]. The intervention was represented as a monthly, slow-release glucocorticoid exposure, consistent with the clinical protocol in which dexamethasone is encapsulated into autologous erythrocytes and released over approximately four weeks following each infusion. Mechanistically, the treatment layer acted by transiently suppressing key pro-inflammatory mediators (primarily IL-6, IL-8, and TNF-α), dampening downstream immune activation loops, and indirectly reducing cytokine-driven neuronal damage. Importantly, the implementation was intentionally constrained to reflect current biological understanding: the intervention modulated downstream inflammatory processes without correcting the upstream ATM defect or restoring lymphocyte development and genomic stability.

Across the 100-patient virtual cohort, UISS-AT predicted that this mechanism would yield partial and short-lived benefits that fail to translate into a robust population-level clinical effect. Each simulated infusion produced a reduction in inflammatory burden and a modest, transient stabilization of immune-cell dynamics; however, these effects decayed between treatment cycles, and the underlying pathological drivers (impaired DNA damage response, restricted adaptive repertoire, immunosenescence, and baseline Purkinje-cell vulnerability) remained active, as reflected by the transient immune stabilization and lack of sustained clinical benefit (Figure 12).

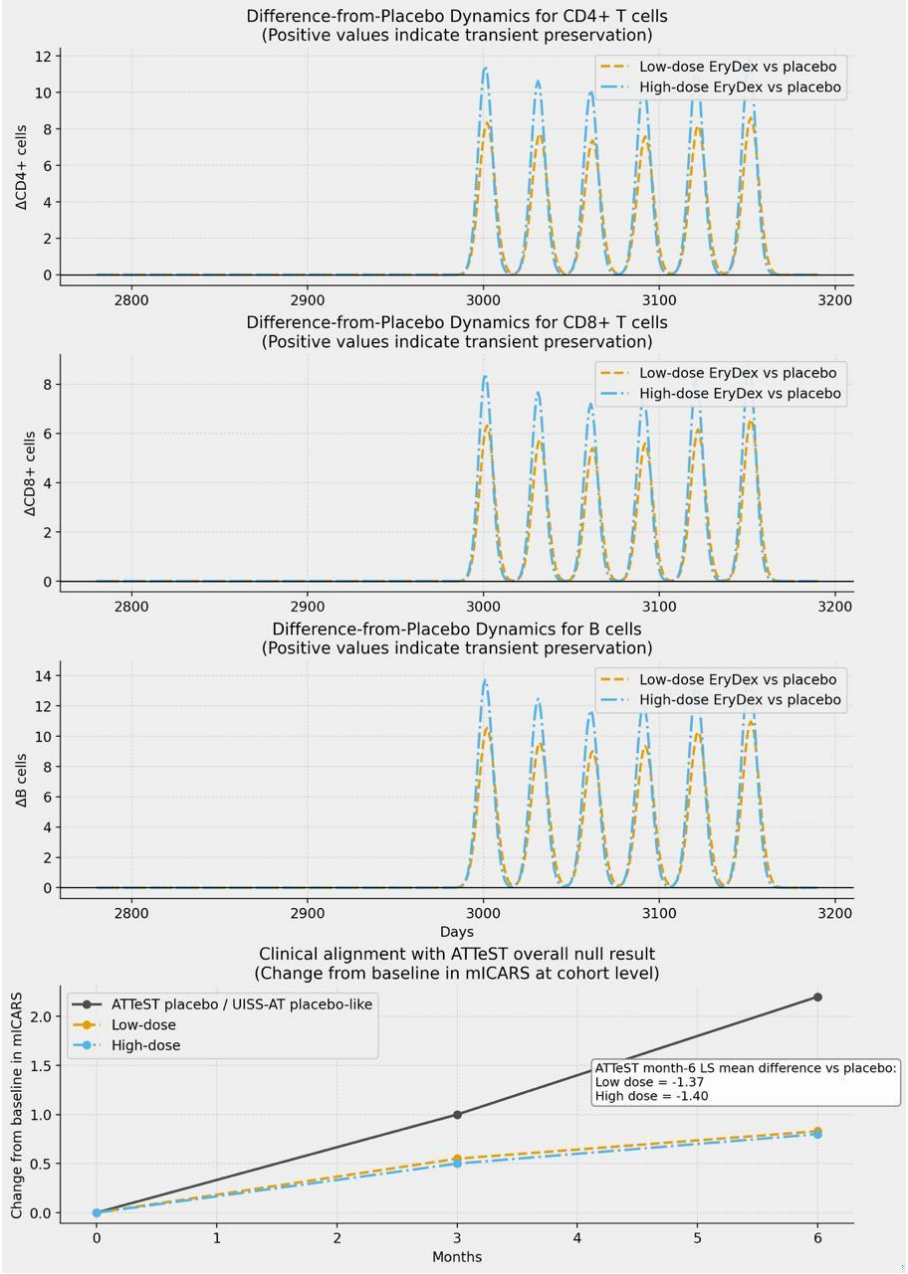

Figure 16 - Difference-from-placebo dynamics for CD4+ T cells, CD8+ T cells, and B cells show modest and short-lived preservation under treatment, with rapid return toward placebo-like behaviour between dosing cycles. The lower panel aligns the simulated cohort-level neurological output with the overall ATTeST finding, in which neither low-dose nor high-dose intra-erythrocyte dexamethasone achieved a statistically significant improvement versus placebo in the modified intention-to-treat population at 6 months. Together, these results show that UISS-AT reproduces a biologically active yet clinically insufficient treatment response.

As a consequence, the cumulative trajectory of neurological decline showed only a limited separation from placebo over the 6-month simulation horizon (Figure 13).

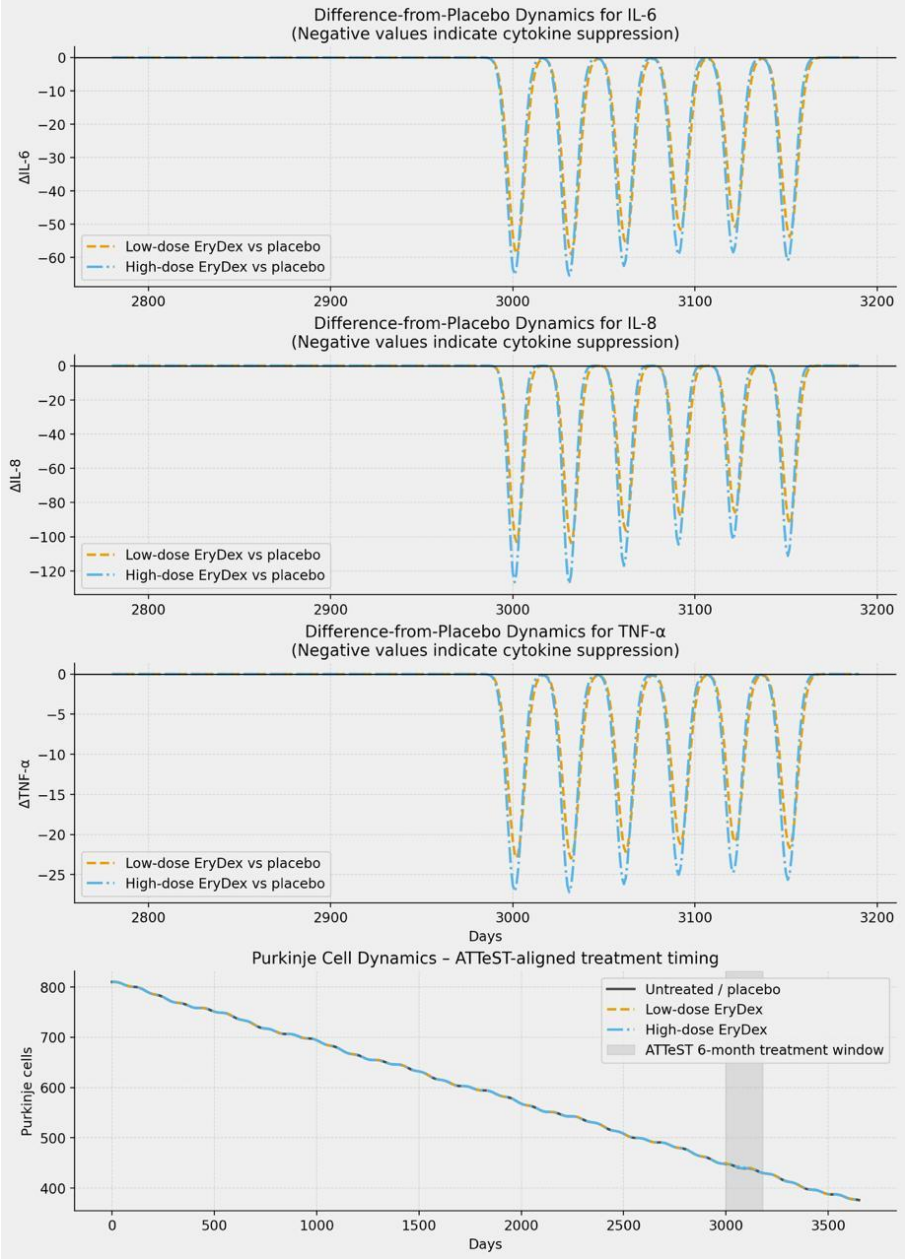

Figure 17 - Difference-from-placebo trajectories for IL-6, IL-8, and TNF-α show repeated transient cytokine suppression following monthly intra-erythrocyte dexamethasone administrations, consistent with short-lived pharmacodynamic activity. However, when the same treatment window is mapped onto long-term Purkinje-cell dynamics, treated and untreated trajectories remain closely superimposable, indicating that transient control of inflammation does not alter the overall neurodegenerative trajectory. This pattern provides a mechanistic interpretation of the overall null efficacy result observed in ATTeST.

This behaviour closely mirrors the ATTeST results, in which no statistically significant improvement in mICARS was observed in the overall modified intention-to-treat population despite measurable biological activity of the treatment.

Beyond reproducing the overall null result, UISS-AT also captured the conditional and context-dependent nature of the treatment response reported in the trial. In ATTeST, signals of efficacy

emerged in more controlled conditions—specifically in the per-protocol population and in younger patients aged 6–9 years—suggesting sensitivity to treatment regularity and disease stage. The same pattern emerged in the simulations: when dosing was delivered consistently and applied earlier in the disease trajectory, the model produced a modest but detectable improvement in neurological outcomes; conversely, when treatment was irregular or applied at more advanced stages, the effect was attenuated and converged toward placebo. This alignment indicates that UISS-AT is able not only to reproduce treatment effects, but also to mechanistically explain their limitations, highlighting the fundamental constraint that anti-inflammatory modulation cannot overcome the primary ATM-dependent disease mechanisms.

Integrated Disease and Treatment Dynamics Support the Biological Plausibility and Credibility of UISS-AT

The simulation results collectively demonstrate that UISS-AT captures both the natural history of AT and the mechanistically consistent effects of anti-inflammatory interventions within a unified framework. In untreated conditions, the disease layer generated coordinated trajectories of immunodeficiency, chronic inflammation and progressive Purkinje-cell loss. When treatment was introduced, the model reproduced cytokine suppression, partial stabilization of immune-cell dynamics and attenuation of inflammation-driven neuronal damage.

Importantly, UISS-AT successfully reproduced multiple independent clinical scenarios involving EryDex treatment, including short-term treatment response [49], long-term treatment continuation and discontinuation [50], and the overall limited efficacy observed in the phase III ATTeST trial [51]. These simulations were not calibrated to force agreement with specific clinical outcomes but emerged from the interaction between the independently implemented disease and treatment layers.

A particularly relevant finding is the model's ability to reproduce the decoupling between biological activity and clinical efficacy observed in the ATTeST study. Although treatment consistently induced measurable reductions in pro-inflammatory cytokines and transient stabilization of immune dynamics, these effects did not translate into a durable modification of the neurodegenerative trajectory. This behaviour emerged naturally from the model structure, in which downstream inflammatory modulation cannot fully compensate for the persistent upstream drivers of disease, including defective DNA damage response, restricted adaptive immune repertoire and progressive immunosenescence.

The interaction between disease and treatment layers therefore follows a coherent causal chain: cytokine suppression reduces inflammatory pressure, reduced inflammatory pressure transiently slows immune and neuronal decline, and the overall effect remains limited in duration and

magnitude because the underlying ATM-dependent pathology remains unchanged. The same mechanistic framework was able to explain both the favourable outcomes reported in early EryDex studies and the more limited efficacy observed in the larger phase III trial.

Collectively, these findings support both the biological plausibility and the credibility of UISS-AT. The ability to reproduce distinct clinical scenarios—including treatment initiation, treatment continuation, treatment discontinuation, varying durations of glucocorticoid exposure and both positive and negative clinical outcomes—strengthens confidence in the model and supports its future use for virtual cohort studies, treatment optimization analyses, verification and validation activities, and model-informed drug development in AT.

Discussion

UISS-AT was developed to provide a mechanistic in silico representation of AT that integrates immune deficiency, chronic inflammation and neurodegenerative progression within a single agent-based framework. The simulations reported here show that the model recapitulates the major pathological axes of AT at the level of a 100-patient virtual cohort: progressive T- and B-cell decline, chronic elevation of pro-inflammatory cytokines and steady Purkinje-cell loss over a 10-year horizon. When a betamethasone treatment layer was superimposed on the disease model, UISS-AT reproduced transient, regimen-dependent reductions in inflammatory burden together with modest temporary stabilization of lymphocyte and Purkinje-cell trajectories. Taken together, these findings support the biological plausibility of the model and suggest that UISS-AT can serve as an integrative platform for studying disease mechanisms and therapeutic modulation in AT.

To our knowledge, UISS-AT represents one of the first mechanistic agent-based frameworks specifically developed to integrate immune dysfunction, chronic inflammation and neurodegeneration in AT. Unlike previous applications in adult immune-mediated neurological diseases, AT provides a distinct setting in which defective ATM-dependent pathways perturb immune development, inflammatory regulation, and neuronal vulnerability from early life. UISS-AT therefore offers a computational architecture to investigate the interdependence among these three pathological axes, as well as their modulation by treatment.

Reduced thymic and bone marrow output, impaired lymphocyte maturation, restricted adaptive repertoire and progressive immunosenescence collectively generate a fragile immune system with limited regenerative capacity. Chronic cytokine dysregulation further sustains a pro-inflammatory environment that amplifies tissue injury and progressively alters immune homeostasis. By linking elevated TNF-α and IL-6 to progressive Purkinje-cell depletion, the model formalizes a biologically meaningful bridge between immune dysfunction and cerebellar degeneration.

Importantly, these interactions unfold during childhood, when both immune competence and cerebellar circuitry are still undergoing maturation. This consideration may also have implications for the interpretation of treatment effects. In the present study, therapeutic interventions were initiated at approximately 8 years of age, a developmental stage in which cerebellar maturation, synaptic refinement, and cerebello-cortical circuit organization are still ongoing. Therefore, treatment effects observed in the simulations may reflect not only attenuation of neurodegenerative processes but also modulation of altered developmental trajectories. This possibility cannot be directly addressed by the current implementation and warrants dedicated investigation in future studies.

Consequently, disease progression in AT may reflect not only progressive tissue degeneration but also altered developmental trajectories arising from the interaction between ATM dysfunction, chronic inflammation and impaired homeostatic regulation.

In this respect, UISS-AT may be viewed not only as a simulator of disease progression, but also as a framework for exploring how ATM dysfunction reshapes the developmental trajectories of interconnected immune and neurological systems. Unlike many chronic disorders in which pathology emerges after maturation has been completed, AT affects both a developing immune system and a developing cerebellum. Consequently, the neurological phenotype may emerge from the interaction between developmental and degenerative processes rather than from neurodegeneration alone. By explicitly linking immune dysfunction, chronic inflammation and neuronal vulnerability, UISS-AT provides a mechanistic platform for investigating how ATM deficiency influences the long-term co-evolution of these systems throughout childhood and adolescence.

This systems-level organization suggests that disease progression in AT may be driven not by the isolated failure of individual biological compartments, but by the progressive destabilization of interconnected immune and neurological homeostatic mechanisms.

The nervous system component of UISS-AT should therefore not be interpreted solely as a marker of neurodegeneration. Although Purkinje-cell loss was selected as a tractable endpoint of cerebellar dysfunction, the simulated neurological trajectory may also reflect the cumulative impact of ATM dysfunction, chronic inflammation and altered developmental processes acting on the immature cerebellum.

The betamethasone simulations further support this interpretation. In the model, glucocorticoid exposure reduces TNF-α, IL-6 and IL-8 during treatment periods, partially attenuates abnormal immune activation and indirectly slows Purkinje-cell loss by reducing inflammatory burden. Consistent with the results shown in Figures 12 and 13, however, these effects remain transient and fail to produce a sustained modification of disease trajectory. This finding suggests that partial

suppression of inflammatory signalling alone is insufficient to overcome the broader ATM-dependent pathological network driving disease progression.

Rather than representing a model failure, this behaviour reinforces the biological plausibility of UISS-AT. If betamethasone had produced durable normalization of lymphocyte counts or complete arrest of neurodegeneration, the model would have implied a correction of disease-driving mechanisms that remain active in AT. Instead, the model preserves the distinction between transient modulation of downstream inflammatory pathways and persistent ATM-dependent pathology. In this respect, UISS-AT captures not only treatment response, but also the mechanistic limits of that response.

The regimen-dependent behaviour is also noteworthy. Although all tested schedules produced measurable benefits, annual pulse regimens resulted in the greatest preservation of Purkinje cells and the most consistent stabilization of B-cell trajectories. These findings suggest that UISS-AT is sufficiently sensitive to discriminate biologically meaningful differences among treatment schedules and to translate them into distinct long-term system behaviours. While not intended to identify an optimal therapeutic strategy, the model provides a mechanistic framework for exploring how treatment timing and frequency may influence disease evolution.

From a broader perspective, this study illustrates how mechanistic in silico modelling can be operationalized in rare multisystem disorders such as AT. The disease arises from dysfunction of the ATM protein, a central regulator of numerous interconnected cellular pathways, giving rise to marked clinical heterogeneity, complex immune-neurological interactions and limited availability of long-term interventional datasets. Under these conditions, purely data-driven approaches often struggle, whereas mechanistic models can add value by integrating fragmented biological and clinical evidence into a formal system that can be queried, perturbed and stress-tested. UISS-AT does not replace experimental or clinical studies, of course, but it offers a structured way to organize current knowledge, test treatment hypotheses and identify candidate mechanisms driving disease progression. Importantly, the use of a 100-patient digital cohort allowed us to move beyond single-trajectory simulations and capture the average system-level behaviour emerging from stochastic variability. This approach increases the robustness of the conclusions and represents a step toward population-level reasoning rather than anecdotal simulation.

Some aspects of the current model should be considered when interpreting these findings. First, model validation is currently retrospective and based primarily on concordance with biological and clinical patterns reported in the literature. UISS-AT reproduces key features of A-T, including lymphopenia, chronic cytokine elevation, progressive Purkinje-cell loss, and transient betamethasone-associated effects; however, these findings should not be interpreted as prospective predictive validation. Such validation remains particularly challenging in AT because of the rarity of the disease, limited longitudinal datasets and substantial clinical heterogeneity. At this current stage, UISS-AT should therefore be regarded as biologically plausible and sufficiently structured

supporting future formal verification, validation and credibility assessment rather than prospective clinical decision-making.

Second, the neurological component of the model remains intentionally simplified. Although Purkinje-cell decline provides a biologically relevant surrogate of cerebellar dysfunction, the current implementation does not explicitly represent the broader cellular and developmental complexity of the cerebellum. In particular, microglial and astrocytic responses, blood–brain barrier dynamics, cerebellar circuitry and detailed compartmentalization of the central nervous system are not explicitly modelled. Neurodegenerative progression is instead represented through a reduced-form neuroimmune framework in which inflammatory mediators contribute to neuronal vulnerability and loss.

An additional limitation is that the model does not explicitly account for postnatal cerebellar development. Because AT manifests during childhood, ATM dysfunction, chronic inflammation, and neurodegenerative processes unfold while cerebellar circuits are still undergoing maturation and refinement. Consequently, the current implementation cannot distinguish between impaired developmental trajectories and subsequent neurodegenerative progression, both of which may contribute to the neurological phenotype of AT.

Third, the betamethasone module remains pharmacodynamically simplified. The model captures the expected anti-inflammatory effects of glucocorticoid exposure and their downstream effects on immune and neurological trajectories, but it does not yet include explicit pharmacokinetics, tissue-specific distribution, receptor saturation, inter-individual differences in steroid responsiveness, or long-term treatment toxicity. For the purposes of the present study, this level of abstraction was sufficient to examine whether the platform could reproduce the transient qualitative pattern of response reported in AT. Nevertheless, a more detailed treatment representation will be necessary if the model is to be extended toward dose optimization or comparative therapeutic design.

Finally, although simulations were performed in a virtual cohort, results are mainly presented as cohort-average trajectories. This provides a robust summary of overall model behaviour, but it does not yet exploit the full potential of the framework to investigate inter-individual variability, mechanistic subgroups, or differential treatment responsiveness. Future developments should therefore place greater emphasis on heterogeneity-aware analyses and stratified virtual populations.

Despite these limitations, the present study demonstrates that UISS-AT can reproduce key features of AT progression while preserving the mechanistic relationships linking immune-inflammatory-neurodegenerative process. Importantly, the model captures transient, clinically plausible glucocorticoid responses without obscuring the underlying ATM-dependent processes that continue to drive disease evolution.

More broadly, UISS-AT opens a mechanistic window onto selected pathogenic processes in AT, without claiming to capture the full complexity of ATM-dependent biology. This is particularly relevant because preclinical and molecular studies indicate that ATM dysfunction perturbs a broad network of interconnected pathways, giving rise to a disease that is intrinsically systemic rather than purely neurological.

However, by providing a unified framework in which selected pathogenic processes can be explored dynamically, UISS-AT offers a foundation for investigating how ATM dysfunction shapes disease trajectories across interconnected biological systems throughout life.

In this sense, the current work is best viewed not as a final model, but as a sufficiently mature computational framework on which more rigorous validation, heterogeneity-aware simulations and additional therapeutic scenarios can now be built.

Such developments may ultimately contribute to broader model-informed approaches for therapeutic evaluation in rare diseases.

Conclusion

UISS-AT provides a mechanistic agent-based representation of AT that captures key features of disease progression and reproduces clinically plausible responses to betamethasone within a virtual patient cohort.

More broadly, UISS-AT should be viewed as a mechanistic representation of selected pathogenic processes in AT rather than a comprehensive representation of ATM-dependent disease biology. While the model captures interactions among immune dysfunction, inflammatory signalling, and neurodegenerative progression, many other ATM-dependent pathways that contribute to the multisystem phenotype of AT remain beyond its current scope.

Future work will focus on formal credibility assessment, sensitivity and uncertainty analyses, heterogeneity-aware simulations, and the extension of the platform to additional therapeutic strategies. Importantly, future simulations should also explore earlier developmental windows. In the current study, treatment was initiated at approximately 8 years of age; however, modelling intervention at earlier stages, such as 3-4 years of age, may help determine whether earlier therapeutic intervention can more effectively influence neurodevelopmental and neurodegenerative trajectories. This would further exploit the potential of UISS-AT to investigate how immune dysregulation, inflammation, and therapeutic interventions interact with cerebellar maturation over time.

Overall, UISS-AT represents a credible and extensible foundation for mechanistic in silico modelling in AT and may support future model-informed therapeutic evaluation in rare diseases.

DECLARATIONS

Ethics approval and consent to participate

Not applicable. This study involved only computational simulations and did not include human participants, identifiable human data, animals, or biological samples.

Consent for publication

Not applicable.

Availability of data and materials

The data generated and analysed during the current study consist of simulation outputs produced by UISS-AT and are included in this article and its supplementary information files. No external datasets were obtained from or downloaded from web-based data banks or repositories for analysis

in this study. Clinical and biological information used to inform and retrospectively assess the model was derived from the published literature cited in the manuscript.

Competing interests

The authors declare no competing interests.

Funding

This work was supported by the European Union under the Horizon Europe research and innovation programme through the ERAMET project (Grant Agreement No. 101137141; call HORIZON-HLTH-2023-IND-06-04 - Modelling and simulation to address regulatory needs in the development of orphan and paediatric medicines). Views and opinions expressed are, however, those of the authors only and do not necessarily reflect those of the European Union or the European Health and Digital Executive Agency (HaDEA). Neither the European Union nor the granting authority can be held responsible for them.

Authors' contributions

G.R. and V.D.S. contributed equally to this work. G.R. contributed to conceptualization, methodology development, formal analysis, interpretation of results, visualization, and writing of the original draft. V.D.S. contributed to data curation, formal analysis, visualization, and manuscript revision. G.N. and A.M. contributed to visualization, and manuscript revision. L.C. contributed to data retrieval and analysis. A.P. provided clinical expertise, contributed to results interpretation, and manuscript revision. F.P. contributed to conceptualization, supervision, project administration, funding acquisition, interpretation of results, and critical revision of the manuscript. All authors reviewed and approved the final manuscript.

References

[1] C. Rothblum-Oviatt, J. Wright, M. A. Lefton-Greif, S. A. McGrath-Morrow, T. O. Crawford, and H. M. Lederman, "Ataxia telangiectasia: a review," *Orphanet J. Rare Dis.*, vol. 11, no. 1, p. 159, Dec. 2016, doi: 10.1186/s13023-016-0543-7.

[2] E. Petley, A. Yule, S. Alexander, S. Ojha, and W. P. Whitehouse, "The natural history of ataxia-telangiectasia (A-T): A systematic review," *PLoS One*, vol. 17, no. 3, p. e0264177, Mar. 2022, doi: 10.1371/journal.pone.0264177.

[3] S. A. McGrath-Morrow *et al.*, "Multidisciplinary Management of Ataxia Telangiectasia: Current Perspectives," *J. Multidiscip. Healthc.*, vol. Volume 14, pp. 1637–1643, Jun. 2021, doi: 10.2147/JMDH.S295486.

[4] P. Amirifar, M. R. Ranjouri, R. Yazdani, H. Abolhassani, and A. Aghamohammadi, "Ataxia-telangiectasia: A review of clinical features and molecular pathology," *Pediatric Allergy and Immunology*, vol. 30, no. 3, pp. 277–288, May 2019, doi: 10.1111/pai.13020.

[5] P. J. McKinnon, “ATM and the Molecular Pathogenesis of Ataxia Telangiectasia,” *Annual Review of Pathology: Mechanisms of Disease*, vol. 7, no. 1, pp. 303–321, Feb. 2012, doi: 10.1146/annurev-pathol-011811-132509.

[6] L. Graafen *et al.*, “Immune profiling and functional analysis of NK and T cells in ataxia telangiectasia,” *Front. Immunol.*, vol. 15, Aug. 2024, doi: 10.3389/fimmu.2024.1377955.

[7] A. Szczawińska-Popłonyk, K. Tąpolska-Jóźwiak, E. Schwartzmann, and B. Pietrucha, “Infections and immune dysregulation in ataxia-telangiectasia children with hyper-IgM and non-hyper-IgM phenotypes: A single-center experience,” *Front. Pediatr.*, vol. 10, Oct. 2022, doi: 10.3389/fped.2022.972952.

[8] A. Rath *et al.*, “A systematic literature review of evidence-based clinical practice for rare diseases: what are the perceived and real barriers for improving the evidence and how can they be overcome?,” *Trials*, vol. 18, no. 1, p. 556, Dec. 2017, doi: 10.1186/s13063-017-2287-7.

[9] J. S. Yu and N. Bagheri, “Agent-Based Models Predict Emergent Behavior of Heterogeneous Cell Populations in Dynamic Microenvironments,” *Front. Bioeng. Biotechnol.*, vol. 8, Jun. 2020, doi: 10.3389/fbioe.2020.00249.

[10] F. Pappalardo, M. Pennisi, and S. Motta, “Universal immune system simulator framework (UISS),” in *Proceedings of the First ACM International Conference on Bioinformatics and Computational Biology*, New York, NY, USA: ACM, Aug. 2010, pp. 649–650. doi: 10.1145/1854776.1854900.

[11] F. Pappalardo *et al.*, “The Potential of Computational Modeling to Predict Disease Course and Treatment Response in Patients with Relapsing Multiple Sclerosis,” *Cells*, vol. 9, no. 3, p. 586, Mar. 2020, doi: 10.3390/cells9030586.

[12] R. Zannolli *et al.*, “A randomized trial of oral betamethasone to reduce ataxia symptoms in ataxia telangiectasia,” *Movement Disorders*, vol. 27, no. 10, pp. 1312–1316, Sep. 2012, doi: 10.1002/mds.25126.

[13] J. H. Steer, K. M. Kroeger, L. J. Abraham, and D. A. Joyce, “Glucocorticoids Suppress Tumor Necrosis Factor-α Expression by Human Monocytic THP-1 Cells by Suppressing Transactivation through Adjacent NF-κB and c-Jun-Activating Transcription Factor-2 Binding Sites in the Promoter,” *Journal of Biological Chemistry*, vol. 275, no. 24, pp. 18432–18440, Jun. 2000, doi: 10.1074/jbc.M906304199.

[14] A. Waage, G. Slupphaug, and R. Shalaby, “Glucocorticoids inhibit the production of IL 6 from monocytes, endothelial cells and fibroblasts,” *Eur. J. Immunol.*, vol. 20, no. 11, pp. 2439–2443, Nov. 1990, doi: 10.1002/eji.1830201112.

[15] S.-H. Kim *et al.*, “Repression of TNF-α-induced IL-8 expression by the glucocorticoid receptor-β involves inhibition of histone H4 acetylation,” *Exp. Mol. Med.*, vol. 41, no. 5, p. 297, 2009, doi: 10.3858/emm.2009.41.5.033.

[16] R. Laubenbacher, F. Hinkelmann, and M. Oremland, “Agent-Based Models and Optimal Control in Biology: A Discrete Approach,” in *Mathematical Concepts and Methods in Modern Biology*, Elsevier, 2013, pp. 143–178. doi: 10.1016/B978-0-12-415780-4.00005-3.

[17] M. Y. Tiet *et al.*, “Biomarkers in Ataxia-Telangiectasia: a Systematic Review,” *J. Neurol.*, vol. 272, no. 2, p. 110, Feb. 2025, doi: 10.1007/s00415-024-12766-7.

[18] E. Cirillo *et al.*, “Progressive Depletion of B and T Lymphocytes in Patients with Ataxia Telangiectasia: Results of the Italian Primary Immunodeficiency Network,” *J. Clin. Immunol.*, vol. 42, no. 4, pp. 783–797, May 2022, doi: 10.1007/s10875-022-01234-4.

[19] A. Szczawińska-Popłonyk, K. Tąpolska-Jóźwiak, E. Schwartzmann, and B. Pietrucha, "Infections and immune dysregulation in ataxia-telangiectasia children with hyper-IgM and non-hyper-IgM phenotypes: A single-center experience," *Front. Pediatr.*, vol. 10, Oct. 2022, doi: 10.3389/fped.2022.972952.

[20] J. Lai *et al.*, "ATM-deficiency-induced microglial activation promotes neurodegeneration in ataxia-telangiectasia," *Cell Rep.*, vol. 43, no. 1, p. 113622, Jan. 2024, doi: 10.1016/j.celrep.2023.113622.

[21] R. Duecker *et al.*, "Hematopoietic Stem Cell Transplantation Restores Naïve T-Cell Populations in Atm-Deficient Mice and in Preemptively Treated Patients With Ataxia-Telangiectasia," *Front. Immunol.*, vol. 10, Nov. 2019, doi: 10.3389/fimmu.2019.02785.

[22] S. A. McGrath-Morrow *et al.*, "Inflammation and transcriptional responses of peripheral blood mononuclear cells in classic ataxia telangiectasia," *PLoS One*, vol. 13, no. 12, p. e0209496, Dec. 2018, doi: 10.1371/journal.pone.0209496.

[23] M. Ambrose and R. A. Gatti, "Pathogenesis of ataxia-telangiectasia: the next generation of ATM functions," *Blood*, vol. 121, no. 20, pp. 4036–4045, May 2013, doi: 10.1182/blood-2012-09-456897.

[24] L. M. Phan and A.-H. Rezaeian, "ATM: Main Features, Signaling Pathways, and Its Diverse Roles in DNA Damage Response, Tumor Suppression, and Cancer Development," *Genes (Basel).*, vol. 12, no. 6, p. 845, May 2021, doi: 10.3390/genes12060845.

[25] Y. Mitiagin and A. Barzilai, "Ataxia-telangiectasia mutated plays an important role in cerebellar integrity and functionality," *Neural Regen. Res.*, vol. 18, no. 3, p. 497, 2023, doi: 10.4103/1673-5374.350194.

[26] F. Cavone *et al.*, "Ataxia Telangiectasia Arising as Immunodeficiency: The Intriguing Differential Diagnosis," *J. Clin. Med.*, vol. 12, no. 18, p. 6041, Sep. 2023, doi: 10.3390/jcm12186041.

[27] A. Giovannetti *et al.*, "Skewed T-cell receptor repertoire, decreased thymic output, and predominance of terminally differentiated T cells in ataxia telangiectasia," *Blood*, vol. 100, no. 12, pp. 4082–4089, Dec. 2002, doi: 10.1182/blood-2002-03-0976.

[28] E. R. Staples *et al.*, "Immunodeficiency in ataxia telangiectasia is correlated strongly with the presence of two null mutations in the ataxia telangiectasia mutated gene," *Clin. Exp. Immunol.*, vol. 153, no. 2, pp. 214–220, Jul. 2008, doi: 10.1111/j.1365-2249.2008.03684.x.

[29] S. Takada *et al.*, "Causative mechanisms and clinical impact of immunoglobulin deficiencies in ataxia telangiectasia," *Journal of Allergy and Clinical Immunology*, vol. 153, no. 5, pp. 1392–1405, May 2024, doi: 10.1016/j.jaci.2023.12.029.

[30] S. Veenhuis, N. van Os, C. Weemaes, E.-J. Kamsteeg, and M. Willemsen, *Ataxia-Telangiectasia*. 1993. [Online]. Available: http://www.ncbi.nlm.nih.gov/pubmed/32791865

[31] B. Reina-San-Martin, H. T. Chen, A. Nussenzweig, and M. C. Nussenzweig, "ATM is required for efficient recombination between immunoglobulin switch regions.," *J. Exp. Med.*, vol. 200, no. 9, pp. 1103–10, Nov. 2004, doi: 10.1084/jem.20041162.

[32] G. J. Driessen *et al.*, "Antibody deficiency in patients with ataxia telangiectasia is caused by disturbed B- and T-cell homeostasis and reduced immune repertoire diversity," *Journal of Allergy and Clinical Immunology*, vol. 131, no. 5, pp. 1367-1375.e9, May 2013, doi: 10.1016/j.jaci.2013.01.053.

[33] T. H. Stracker, I. Roig, P. A. Knobel, and M. Marjanović, "The ATM signaling network in development and disease," *Front. Genet.*, vol. 4, 2013, doi: 10.3389/fgene.2013.00037.

[34] T. J. Weitering, D. Berghuis, M. Blom, M. A. A. P. Willemsen, and M. van der Burg, "Clinical challenges following early detection of ataxia telangiectasia through SCID newborn screening," *Journal of Human Immunity*, vol. 1, no. 4, Nov. 2025, doi: 10.70962/jhi.20250052.

[35] S. A. McGrath-Morrow *et al.*, "Inflammation and transcriptional responses of peripheral blood mononuclear cells in classic ataxia telangiectasia," *PLoS One*, vol. 13, no. 12, p. e0209496, Dec. 2018, doi: 10.1371/journal.pone.0209496.

[36] C. Rothblum-Oviatt, J. Wright, M. A. Lefton-Greif, S. A. McGrath-Morrow, T. O. Crawford, and H. M. Lederman, "Ataxia telangiectasia: a review," *Orphanet J. Rare Dis.*, vol. 11, no. 1, p. 159, Dec. 2016, doi: 10.1186/s13023-016-0543-7.

[37] T. Li and Z. J. Chen, "The cGAS–cGAMP–STING pathway connects DNA damage to inflammation, senescence, and cancer," *Journal of Experimental Medicine*, vol. 215, no. 5, pp. 1287–1299, May 2018, doi: 10.1084/jem.20180139.

[38] R. A. Saunders *et al.*, "Elevated inflammatory responses and targeted therapeutic intervention in a preclinical mouse model of ataxia-telangiectasia lung disease," *Sci. Rep.*, vol. 11, no. 1, p. 4268, Feb. 2021, doi: 10.1038/s41598-021-83531-3.

[39] L. Graafen *et al.*, "Immune profiling and functional analysis of NK and T cells in ataxia telangiectasia," *Front. Immunol.*, vol. 15, Aug. 2024, doi: 10.3389/fimmu.2024.1377955.

[40] J. A. Metcalfe *et al.*, "Accelerated telomere shortening in ataxia telangiectasia," *Nat. Genet.*, vol. 13, no. 3, pp. 350–353, Jul. 1996, doi: 10.1038/ng0796-350.

[41] E. F. Carney, V. Srinivasan, P. A. Moss, and A. M. Taylor, "Classical Ataxia Telangiectasia Patients Have a Congenitally Aged Immune System with High Expression of CD95," *The Journal of Immunology*, vol. 189, no. 1, pp. 261–268, Jul. 2012, doi: 10.4049/jimmunol.1101909.

[42] J. Aguado *et al.*, "Inhibition of the cGAS-STING pathway ameliorates the premature senescence hallmarks of Ataxia-Telangiectasia brain organoids," *Aging Cell*, vol. 20, no. 9, Sep. 2021, doi: 10.1111/acel.13468.

[43] K. R. Choy and D. J. Watters, "Neurodegeneration in ataxia-telangiectasia: Multiple roles of ATM kinase in cellular homeostasis," *Developmental Dynamics*, vol. 247, no. 1, pp. 33–46, Jan. 2018, doi: 10.1002/dvdy.24522.

[44] X. Song, F. Ma, and K. Herrup, "Accumulation of Cytoplasmic DNA Due to ATM Deficiency Activates the Microglial Viral Response System with Neurotoxic Consequences," *The Journal of Neuroscience*, vol. 39, no. 32, pp. 6378–6394, Aug. 2019, doi: 10.1523/JNEUROSCI.0774-19.2019.

[45] J. Bourseguin *et al.*, "Persistent DNA damage associated with ATM kinase deficiency promotes microglial dysfunction," *Nucleic Acids Res.*, vol. 50, no. 5, pp. 2700–2718, Mar. 2022, doi: 10.1093/nar/gkac104.

[46] G. Giardino *et al.*, "Betamethasone therapy in <scp>a</scp> taxia <scp>t</scp> elangiectasia: unraveling the rationale of this serendipitous observation on the basis of the pathogenesis," *Eur. J. Neurol.*, vol. 20, no. 5, pp. 740–747, May 2013, doi: 10.1111/ene.12024.

[47] T. Broccoletti *et al.*, "Efficacy of very-low-dose betamethasone on neurological symptoms in ataxia-telangiectasia," *Eur. J. Neurol.*, vol. 18, no. 4, pp. 564–570, Apr. 2011, doi: 10.1111/j.1468-1331.2010.03203.x.

[48] I. Russo *et al.*, “In ataxia-teleangiectasia betamethasone response is inversely correlated to cerebellar atrophy and directly to antioxidative capacity,” *Eur. J. Neurol.*, vol. 16, no. 6, pp. 755–759, Jun. 2009, doi: 10.1111/j.1468-1331.2009.02600.x.

[49] L. Chessa *et al.*, “Intra-Erythrocyte Infusion of Dexamethasone Reduces Neurological Symptoms in Ataxia Teleangiectasia Patients: Results of a Phase 2 Trial,” *Orphanet J. Rare Dis.*, vol. 9, no. 1, p. 5, Dec. 2014, doi: 10.1186/1750-1172-9-5.

[50] V. Leuzzi *et al.*, “Positive effect of erythrocyte-delivered dexamethasone in ataxia-telangiectasia,” *Neurol. Neuroimmunol. Neuroinflamm.*, vol. 2, no. 3, Jun. 2015, doi: 10.1212/NXI.0000000000000098.

[51] S. Zielen *et al.*, “Safety and efficacy of intra-erythrocyte dexamethasone sodium phosphate in children with ataxia telangiectasia (ATTeST): a multicentre, randomised, double-blind, placebo-controlled phase 3 trial,” *Lancet Neurol.*, vol. 23, no. 9, pp. 871–882, Sep. 2024, doi: 10.1016/S1474-4422(24)00220-5.

[52] T. Broccoletti *et al.*, “Steroid-induced improvement of neurological signs in ataxia-telangiectasia patients,” *Eur. J. Neurol.*, vol. 15, no. 3, pp. 223–228, Mar. 2008, doi: 10.1111/j.1468-1331.2008.02060.x.